Porifera

4

Bernard M. Degnan, Maja Adamska,
Gemma S. Richards, Claire Larroux, Sven Leininger,
Brith Bergum, Andrew Calcino, Karin Taylor,
Nagayasu Nakanishi, and Sandie M. Degnan

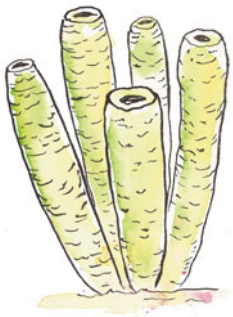

Chapter vignette artwork by Brigitte Baldrian.

B.M. Degnan (✉) • C. Larroux • A. Calcino
K. Taylor • N. Nakanishi • S.M. Degnan
Centre for Marine Science, School of Biological
Sciences, University of Queensland,
Brisbane, QLD 4072, Australia
e-mail: b.degnan@uq.edu.au

M. Adamska • G.S. Richards
Centre for Marine Science, School of Biological
Sciences, University of Queensland,
Brisbane, QLD 4072, Australia

Sars International Centre for Marine Molecular
Biology, University of Bergen,
Thormøhlensgt. 55, Bergen 5008, Norway

S. Leininger
Sars International Centre for Marine Molecular
Biology, University of Bergen,
Thormøhlensgt. 55, Bergen 5008, Norway

Institute of Marine Research,
Nordnesgaten 50, Bergen 5005, Norway

B. Bergum
Sars International Centre for Marine Molecular
Biology, University of Bergen,
Thormøhlensgt. 55, Bergen 5008, Norway

Faculty of Medicine and Dentistry, University
of Bergen, P.O. Box 7804, Bergen 5020, Norway

A. Wanninger (ed.), *Evolutionary Developmental Biology of Invertebrates 1: Introduction, Non-Bilateria, Acoelomorpha, Xenoturbellida, Chaetognatha*
DOI 10.1007/978-3-7091-1862-7_4, © Springer-Verlag Wien 2015

INTRODUCTION

Poriferans (sponges) are sessile aquatic (largely marine) animals that are found in almost all benthic habitats. There are an estimated 15,000 species living today, although many have not been described (reviewed in Hooper and Van Soest 2002). The sponge body plan is amongst the simplest in the animal kingdom and lacks nerve and muscle cells and a centralised gut (reviewed in Simpson 1984; Ereskovsky 2010; Leys and Hill 2012). Their body plan and ecology, and thus their evolution, appear to be intimately associated with the diversity of microbial symbionts they harbour (reviewed in Hentschel et al. 2012; Thacker and Freeman 2012), as is the case with other metazoans (McFall et al. 2013).

Sponges are separated from the external environment by an epithelial layer, the exopinacoderm. External pores in this outer boundary connect to an internal network of canals and chambers, which are lined by epithelial endopinacocytes and ciliated choanocytes, respectively. Choanocyte chambers pump water through this internal aquiferous canal system, drawing food into the sponge. This current also fulfils most of the sponge's physiological requirements, including respiration and excretion. Between the internal and external epithelial layers is the collagenous mesohyl, which is enriched with multiple cell types, often including pluripotent archaeocytes and skeletogenic sclerocytes that fabricate siliceous or calcareous spicules (Fig. 4.1). This juvenile/adult body plan is typically the outcome of the dramatic reorganisation of a radially symmetrical, bi- or trilayered larva at metamorphosis. Metamorphosis is deemed to be complete when the functional feeding juvenile is formed. This so-called rhagon or olynthus stage has been proposed to be the phylotypic stage for demosponges and calcisponges, respectively (reviewed in Ereskovsky 2010). It is often cited that poriferans lack true tissue-level organisation; however, there are numerous examples of tissue- and organ-like structures and functionalities in both larval and adult forms (e.g., the photosensitive pigment ring of many larvae).

Phylogenetic Position of Porifera

Porifera is traditionally regarded as the oldest surviving phyletic lineage of animals and in the past was often relegated into its own subkingdom, the Parazoa. Recent molecular phylogenetic analyses however have put forward a range of alternative proposals that either support

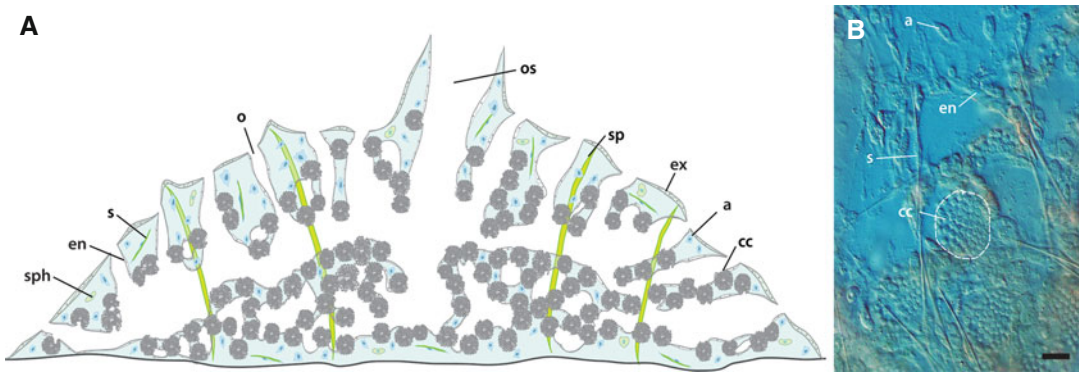

Fig. 4.1 Juvenile poriferan body plan. (**A**) Diagram of a sponge with leuconoid aquiferous system. Water flows into the internal aquiferous system via the ostium and out via the osculum. The mesohyl is shown in blue and populated by archaeocytes and other cell types, including sclerocytes and spherulous cells. (**B**) Optical section of a 3-day-old *Amphimedon queenslandica* juvenile showing internal morphology. Archeocyte (*a*), choanocyte chamber (*cc*), endopinacoderm (*en*), exopinacoderm (*ex*), ostium (*o*), osculum (*os*), sclerocyte (*s*), spicule (*sp*), and spherulous cell (*sph*). Scale bar: 10 μm

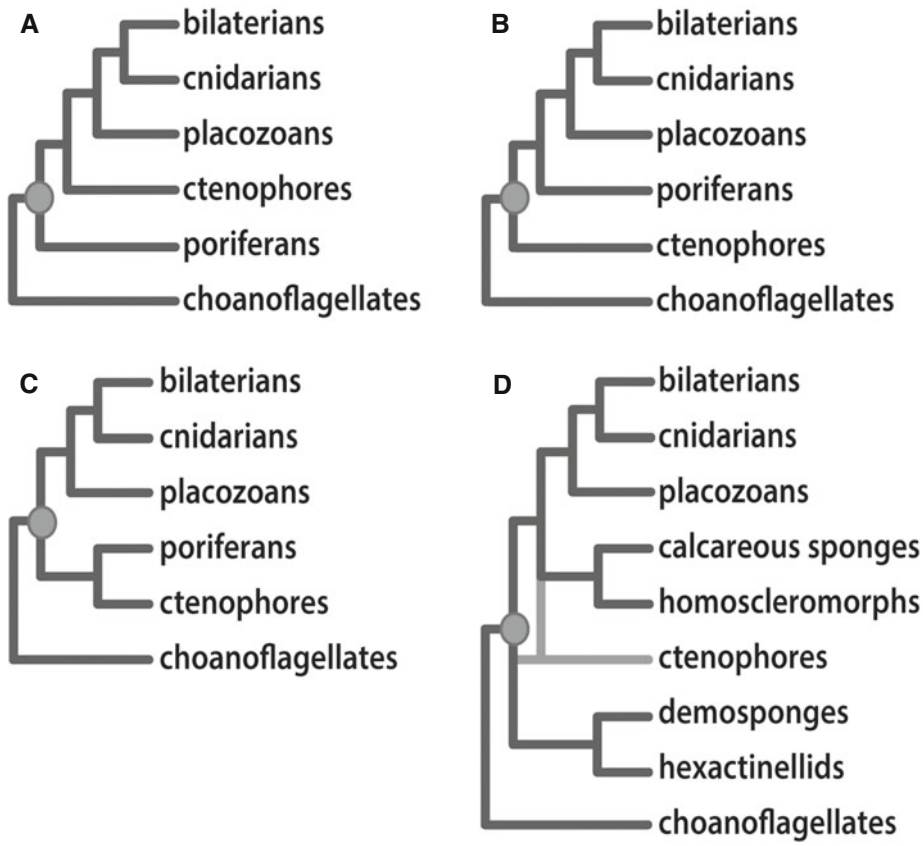

Fig. 4.2 Phylogenetic position of Porifera. Four hypotheses of the inter- and intrarelationship of sponges. These trees are largely derived from, and supported by, recent phylogenomic datasets. The grey node in each tree represents the last common ancestor to contemporary metazoans. (**A**) Porifera as the earliest branching metazoan phyletic lineage and sister to the Eumetazoa (Ctenophora, Placozoa, Cnidaria, and Bilateria); one possible tree topology is shown (Phillipe et al. 2009). (**B**) Ctenophora as the earliest branching metazoan phyletic lineage (Ryan et al. 2013; Moroz et al. 2014). (**C**) Porifera and Ctenophora form a clade separate from Placozoa, Cnidaria, and Bilateria. Recent detailed phylogenomic analyses raise the possibility that sponges and ctenophores may be sister taxa. This hypothesis is supported by the striking similarity of the developmental gene repertoires of the demosponge *Amphimedon queenslandica* and ctenophores. (**D**) Paraphyletic sponges with classes Calcarea and Homoscleromorpha more closely related to the Eumetazoa than to classes Demospongiae and Hexactinellida (Sperling et al. 2009); Ctenophora unresolved in this hypothesis. Note that hypotheses that place placozoans in the most basal position within the Metazoa or within a clade consisting of them, sponges, cnidarians, and ctenophores (e.g., Schierwater et al. 2009), are consistently rejected based on current genomic and transcriptomic data and thereby not included in this figure

(e.g., Philippe et al. 2009; Srivastava et al. 2010) or reject this traditional view (Fig. 4.2; e.g., Schierwater et al. 2009; Sperling et al. 2009; Ryan et al. 2013; Moroz et al. 2014). Specifically, current points of debate are whether poriferans or ctenophores are the sister group to all other animals and whether sponges are monophyletic. Thus, interpretations of the sponge body plan in the context of metazoan evolution range from it representing a state similar to the last common ancestor (LCA) of contemporary metazoans to it being derived from a morphologically more complex LCA that possessed a gut, nerves, and muscles.

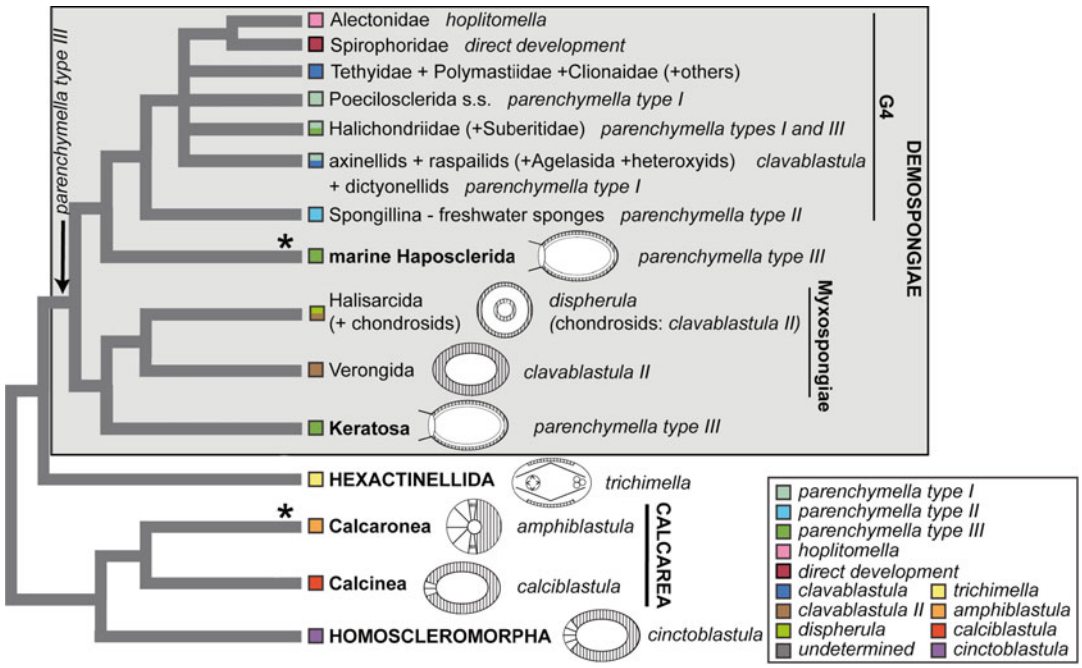

Fig. 4.3 Larval types mapped onto a recently proposed poriferan phylogeny. Stars mark lineages that include the demosponge *Amphimedon queenslandica* and calcareous sponge *Sycon ciliatum* (Figure adapted from Worheide et al. (2012))

Phylogenetic Relationships of Poriferan Classes

Classes Demospongiae, Calcarea, Homoscleromorpha, and Hexactinellida comprise phylum Porifera, with the Demospongiae being by far the most speciose. There is a growing consensus that demosponges and hexactinellids (sponges with a syncytial body organisation) and calcisponges and homoscleromorphs form pairs of sister classes (Fig. 4.3; Philippe et al. 2009; Gazave et al. 2012; Woerheide et al. 2012; Hill et al. 2013; Redmond et al. 2013; Thaker et al. 2013). However, there currently exist two broad views as to the exact relationship of these classes, one in which they form a monophyletic phylum (e.g., Philippe et al. 2009) and another where a clade comprised of demosponges and hexactinellids are separate from a clade comprised of calcisponges and homoscleromorphs + eumetazoans (Fig. 4.3; e.g., Sperling et al. 2009). Regardless, it appears that these classes diverged from each other over 600 million years ago, well before eumetazoan cladogenesis and the Cambrian explosion (Erwin et al. 2011).

Developmental Commonalities Within the Porifera

Poriferans exhibit a wide range of embryonic and larval types that are formed through a diversity of morphogenetic processes, many of which appear similar to those used during bilaterian development (Figs. 4.3 and 4.4). For instance, morphogenetic mechanisms, such as cell delamination (e.g., the hexactinellid *Oopsacas minuta*; Boury-Esnault et al. 1999), ingression (e.g., the halisarcid *Halisarca dujardini*; Gonobobleva and Ereskovsky 2004), egression (e.g., the homoscleromorph *Oscarella* sp.; Ereskovsky and Boury-Esnault 2002), and invagination (e.g., the halisarcid *Halisarca dujardini*; Gonobobleva and Ereskovsky 2004), are employed during sponge embryogenesis, albeit often in a taxon-restricted manner. For detailed descriptions of sponge

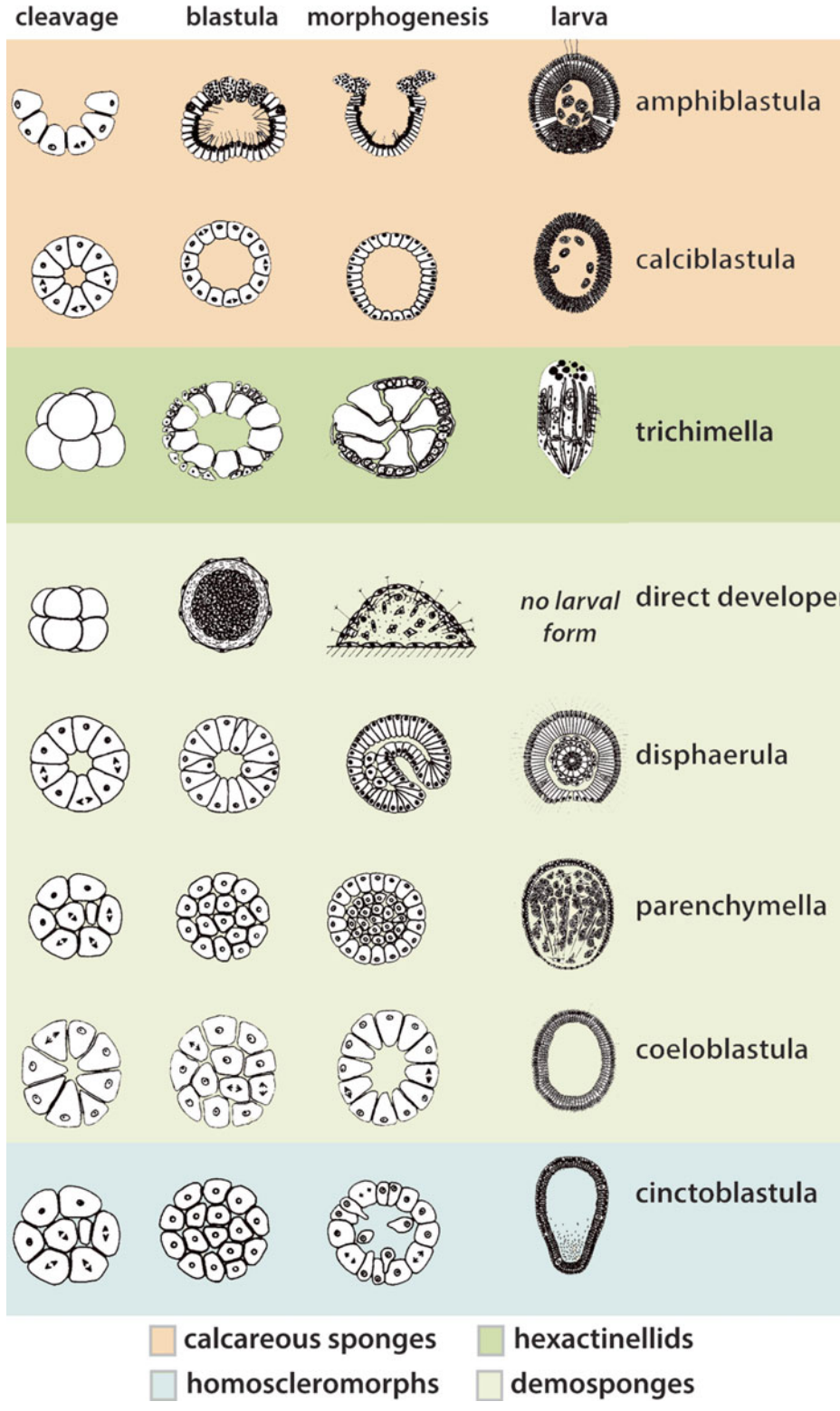

Fig. 4.4 Summary of the modes of poriferan development (Figure adapted from Ereskovsky (2010))

development, the reader is directed to the recent excellent and scholarly book by Ereskovsky (2010) and other reviews (e.g., Leys 2004; Leys and Ereskovsky 2006; Leys and Hill 2012).

Regardless of the differences in external characteristics of different sponge embryos, larvae, postlarvae, juveniles, and adults (see Figs. 4.3 and 4.4), poriferan development employs a similar morphogenetic toolkit to that used by more complex animals. These fundamental features of development result from the spatiotemporal regulation of gene expression and include the establishment of differential cell affinities, cell type-specific movements, and structural changes and the regulation of cell proliferation and death. As we will see in later sections, the localised expression of transcription factor genes is likely to play a central role in establishing differential patterns of gene expression in sponges, just as it does in more complex animals. Further, mechanisms such as asymmetric cell division, cytoplasmic determinants, and intracellular signalling probably contribute to the specification and determination of cell identity in sponges. Other symmetry-breaking processes, such as morphogen gradients, also appear necessary for the formation of the poriferan body plan.

It is well accepted that multilayered poriferan body plans form through a series of morphogenetic processes underpinned by a combination of differential cell affinities and movements, but it remains a point of debate as to whether sponges gastrulate or possess germ layers (e.g., Leys 2004; Ereskovsky 2010; Leininger et al. 2014; Nakanishi et al. 2014). Perhaps less contentious, most morphogenetic movements in sponges can be viewed in the context of epithelial and mesenchymal cell behaviours and interactions. That is, during the course of development, sponge cells can operate semi-autonomously or in partially or fully integrated layers and have the capacity to migrate into or from a cell layer as an individual or a group (reviewed in Ereskovsky 2010).

With few exceptions, sponges have a biphasic pelagobenthic life cycle with a tiny, planktonic ciliated larva that metamorphoses and grows into a large, benthic adult that is sexually reproductive (Degnan and Degnan 2006, 2010; Ereskovsky 2010). The body plans of a majority of sponges continually undergo remodelling and regeneration throughout their life although this is less pronounced in some calcisponges (e.g., *Sycon ciliatum*). Thus, the morphogenetic mechanisms and processes outlined above, along with the processes of transdifferentiation and apoptosis, are operational throughout the life of most sponges (Ereskovsky 2010; Funayama 2012; Nakanishi et al. 2014). This also applies to asexual reproduction, which is not covered in this chapter.

The Demosponge *Amphimedon queenslandica* and the Calcareous Sponge *Sycon ciliatum*

As outlined above, sponge development is as varied as in any other phylum, and this chapter does not attempt to cover this diversity. Instead, here we focus on two species for which a majority of developmental gene expression patterns currently exist, the demosponge *Amphimedon queenslandica* and calcareous sponge *Sycon ciliatum*. Analysis of developmental gene expression, combined with experimental analysis of embryogenesis and metamorphosis, provides a means for more detailed and accurate comparisons of sponge and eumetazoan development. Both *A. queenslandica* and *S. ciliatum* have well-annotated draft genomes supported by extensive developmental transcriptomes (Srivastava et al. 2010; Anavy et al. 2014; Leininger et al. 2014). Importantly, these sponges differ markedly in their mechanisms of development. As demosponge and calcareous sponge lineages most likely diverged well before the Cambrian, a comparison of *A. queenslandica* and *S. ciliatum* genomes and development has the potential to provide insights into their common ancestor, which existed over 600 million years ago (Erwin et al. 2011).

The Demosponge *Amphimedon queenslandica*

Amphimedon queenslandica (class Demospongiae, order Haplosclerida, family Niphatidae) is currently the sponge with the most extensive developmental gene expression data. Its draft genome was published in 2010, further enhancing its utility for understanding demosponge development and metazoan evolution. A number of studies have been published about the evolution of metazoan cell types and gene families using *A. queenslandica* (Table 4.3). Akin to other sponges and indeed other animals, development in *Amphimedon queenslandica* progresses through a series of recognisable phases. It begins with the subdivision of the fertilised oocyte into progressively smaller blastomeres, followed by the acquisition of embryonic polarity and the sorting of cells into layers via broad-scale cell migrations. Activity then centres on the patterning and differentiation of diverse cell types in defined localities throughout the embryo and the morphogenesis of larval structures (Fig. 4.6). Differing from typical eumetazoan development in which patterning processes occur before terminal differentiation, embryonic pigment cells, ciliated epithelial cells, and sclerocytes in *A. queenslandica* express terminal differentiation characters, pigment granules, cilia, and spicules, respectively, directly following cleavage. Early differentiation of cells during embryogenesis appears to be a shared feature amongst many sponges.

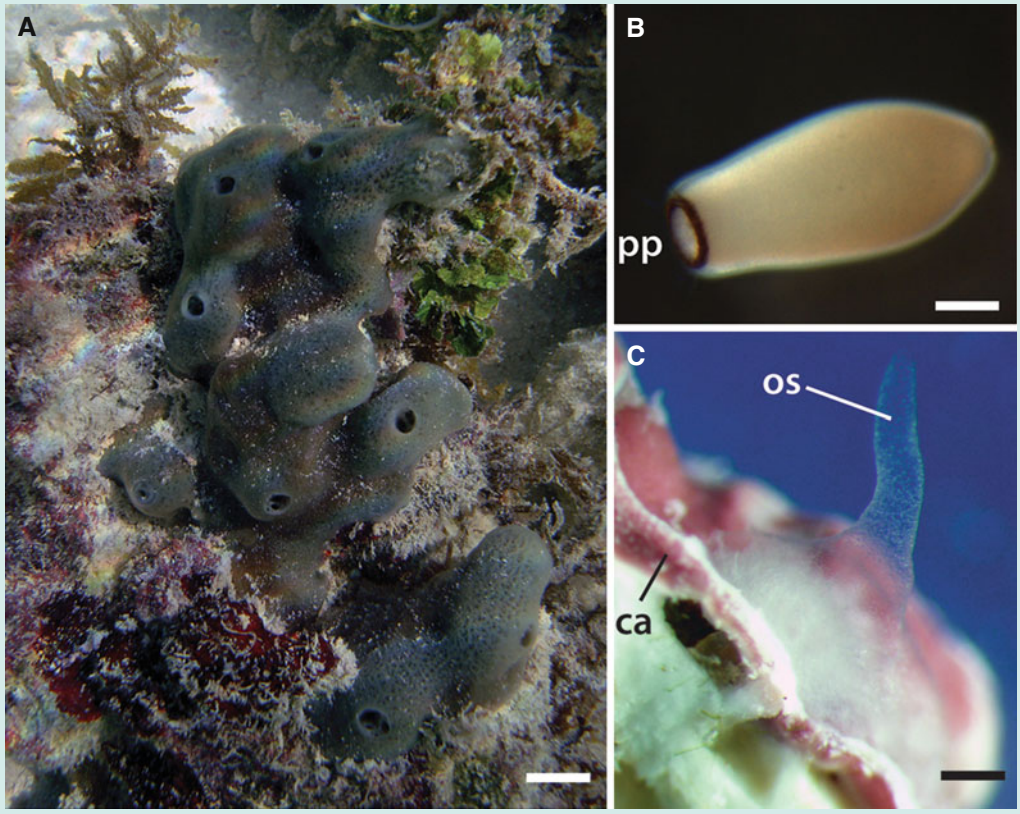

Amphimedon queenslandica. (**A**) Adult in situ on the southern Great Barrier Reef. (**B**) Larva with posterior pigment ring (*pp*) to the *left*. (**C**) A 3-day-old juvenile settled on crustose coralline alga (*ca*) with osculum (*os*) pointed upwards

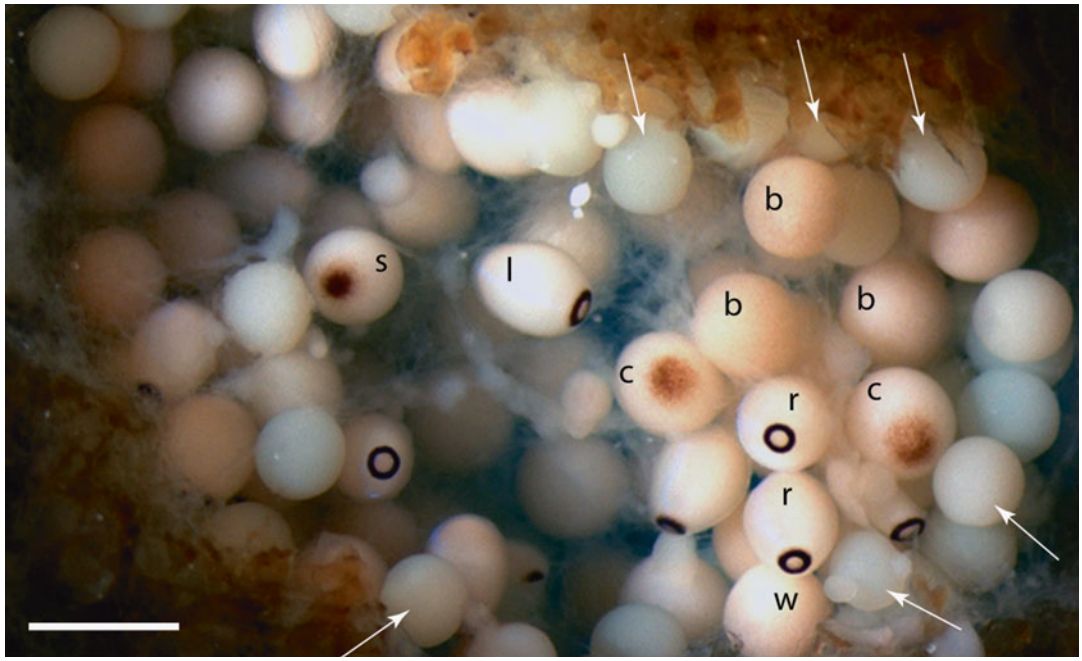

Fig. 4.5 An *Amphimedon queenslandica* brood chamber. Small white and translucent oocytes are located on the outer edge of the brood chamber (*white arrows*), which is surrounded by brown somatic cells. White (*w*), brown (*b*), cloud (*c*), and ring (*r*) stage embryos and unhatched larvae (*l*) are mixed within the chamber. Scale bar: 1 mm

THE *AMPHIMEDON QUEENSLANDICA* BROOD CHAMBER: GAMETOGENESIS AND FERTILISATION

Amphimedon queenslandica is viviparous, and its embryos are concentrated into brood chambers, several of which can occur in a single adult all year round (Fig. 4.5). However, the developmental origins of its gametes are unknown. In other viviparous sponges, oocytes appear to differentiate from either archaeocytes or choanocytes (reviewed in Simpson 1984; Kaye 1990; Ereskovsky 2010). The engulfment of nutrient-laden nurse cells (also called trophocytes/spherulous cells; Simpson 1984; Ereskovsky 2010) is considered an important feature of oogenesis (e.g., Fell 1969; Saller and Weissenfels 1985). Pre-cleavage stages are known to reside at the edges of the brood chambers in *A. queenslandica* and can be identified by their translucent, smaller appearance and flattened shape in comparison to the more spherical and opaque embryos (Fig. 4.5; Leys and Degnan 2001; Adamska et al. 2010). Embryos and unhatched larvae are mixed and located more centrally in the brood chamber, with later stages tending to be towards the middle of the chamber. Developmental stages are identifiable and named by the presence and pattern of pigment cells, which first appear during cleavage: white stage embryos comprise a range of early cleavage stages; brown embryos have pigment cells distributed throughout the embryo and mark the transition from cleavage to the two-layered embryo; cloud stage appears after the anterior-posterior (AP) axis is established, with the pigment cells concentrating towards the future posterior pole; and spot to ring stages are identified by pigment cells concentrated at the posterior pole either as a spot or

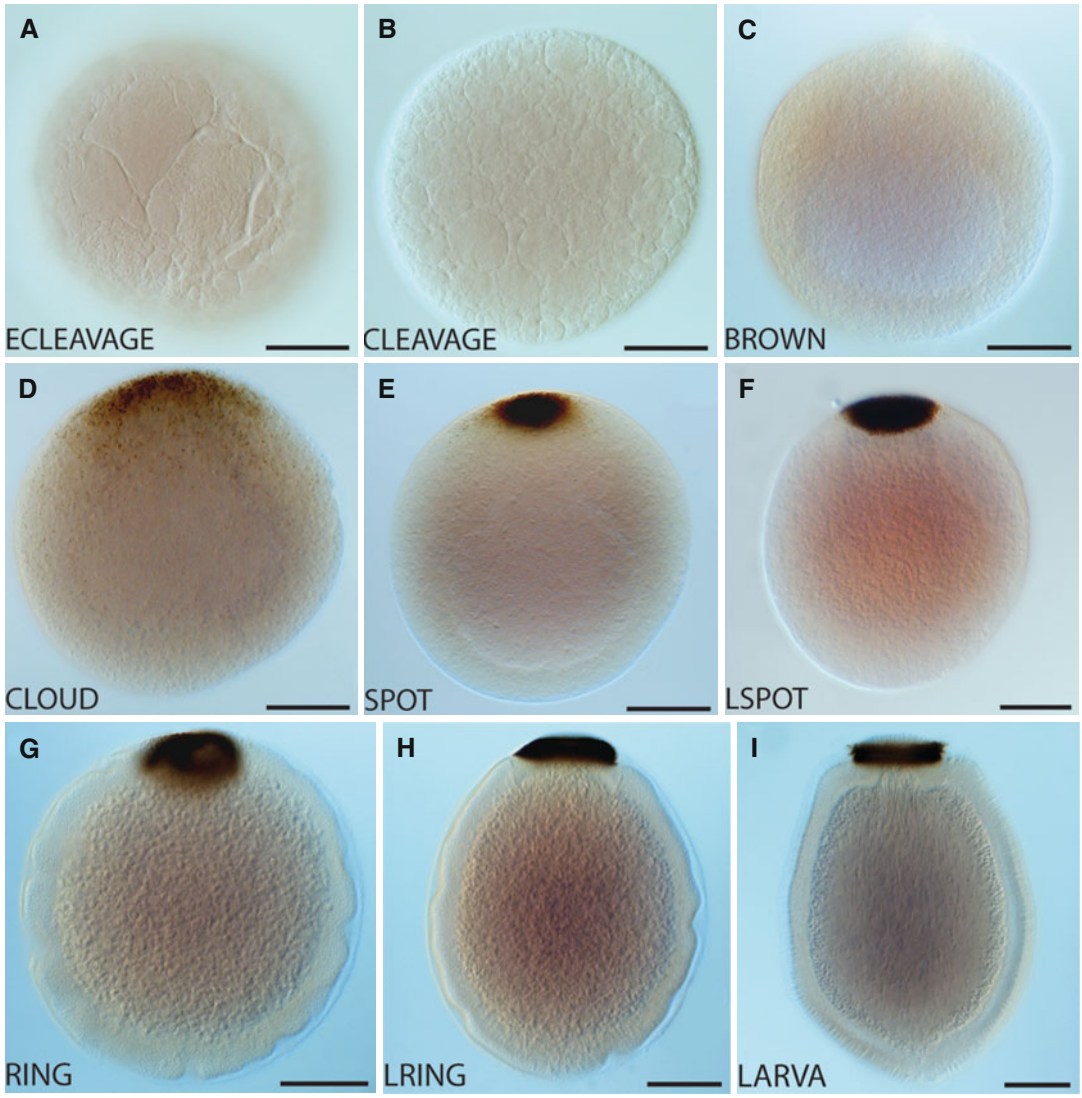

Fig. 4.6 Developmental stages of *Amphimedon queenslandica*. Whole-mount light micrographs of fixed and cleared *Amphimedon queenslandica* embryos and larva. Posterior is to the *top* in (**C–I**); orientation unknown in (**A**, **B**). *E* early, *L* late in (**A**, **F**, **H**). Scale bar: 100 μm

ring – ring stage follows spot stage – and characterised by morphogenesis of specific cell types and tissues (Fig. 4.6).

Like many sponges, *Amphimedon queenslandica* is a hermaphrodite that reproduces by spermcast spawning, followed by the apparent passive uptake by maternal adults of free spermatozoa from what is presumably a very dilute suspension in the water column. Genotyping of microsatellite loci with high allelic diversity (that together yield a combined paternal exclusion probability of 95 %) has revealed that up to 26 different paternal adults can be attributed to progeny being brooded by a single maternal adult at any particular time (Table 4.1). Near neighbours (within 4 m radius) can account for most of the fertilisations, but some progeny appear to be fathered by sperm

Table 4.1 Estimates of minimum number of fathers contributing to the genotypes of brooded embryos in two maternal adults

Maternal adult ID	Nos. embryos genotyped	Nos. potential fathers in 4 m radius in field	Microsatellite locus ID	# paternal alleles	Minimum nos. fathers per maternal adult
A	73	33	MS16	18	~9
			MS34	30	~15
			MS9	22	~11
			MS19	15	~8
			Mean[a]	*21.25 ± 3.25*	*~11*
B	315	17	MS16	37	~19
			MS34	51	~26
			MS9	32	~16
			MS19	22	~11
			Mean[a]	*35.50 ± 6.04*	*~18*

[a]Mean number of paternal alleles across four microsatellite loci ± standard error

Table 4.2 Proportion of embryos at different stages of development in four example maternal adults

	Proportion of each developmental stage						
Maternal adult ID	White	Brown	Cloud	Spot	Ring	Larva	Total nos.
A	0.40	0.18	0.04	0.14	0.16	0.08	73
C	0.24	0.16	0.07	0.13	0.23	0.17	315
B	0.28	0.14	0.07	0.21	0.14	0.16	159
D	0.51	0.11	0.04	0.18	0.16	0.00	107

sourced from a greater distance (Table 4.1). In any particular brood chamber, up to 30 % of white stage embryos appear to be of maternal origin only (i.e., unfertilised). However, as noted below, early cleaving embryos include a large number of maternal nurse cells, which eventually die. The import of these additional maternal genomes may prevent the detection of paternal microsatellite alleles in early embryos by increasing the ratio of maternal to paternal amplifiable DNA.

Although *Amphimedon queenslandica* fecundity is highest in the warmer months of the year, embryos of most developmental stages are present in most brood chambers at most times (Table 4.2). While overall there can be a large number of paternal contributors to fertilisation in a single maternal adult, only a subset of these fathers appear to contribute to any one brood chamber. There is no indication, however, that all embryos at a particular developmental stage within a brood chamber represent a single input of sperm from a single paternal source. Together, these observations suggest that *A. queenslandica* adults maintain a constant supply of all developmental stages, leading to a steady daily release of mature larvae (Maritz et al. 2010), by (i) passively accepting sperm that are trickle released continuously from neighbouring paternal adults and possibly also (ii) active regulation of fertilisation by stored sperm and/or regulation of the initiation or rate of development of fertilised eggs.

EARLY EMBRYONIC DEVELOPMENT IN *AMPHIMEDON QUEENSLANDICA*

Cleavage

Cleaving *Amphimedon queenslandica* embryos (Figs. 4.7, 4.8, 4.9, and 4.10) are similar to other demosponge embryos (Fig. 4.4; Fell 1969; Saller and Weissenfels 1985; De Vos et al. 1991; Kaye and Reiswig 1991; Leys and Ereskovsky 2006; reviewed in Ereskovsky 2010). The entire embryo is enveloped in a layer of squamous follicle cells with large nuclei, presumably of maternal origin (Fig. 4.8; Leys and Degnan 2002). In early cleaving stages, the blastomeres are unequal in size

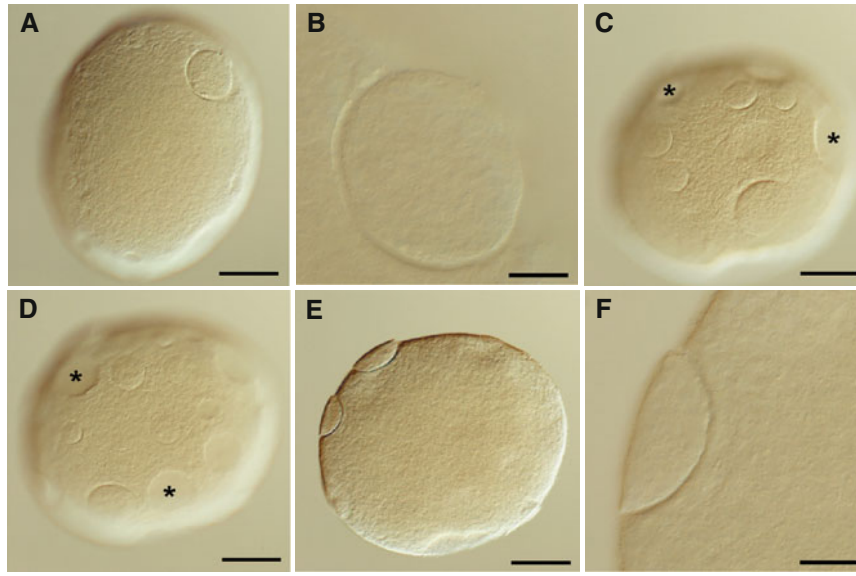

Fig. 4.7 Whole-mount micrographs of very early cleaving *Amphimedon queenslandica* embryos. Optical sections of two fixed and cleared embryos (**A**, **B** and **C**–**F**), from which follicle membranes have been removed. (**A**) A single large macromere has cleaved and is shown in higher magnification in (**B**). (**C**) Multiple large macromeres have cleaved in the second embryo, and several of them have fallen off during preparation of the sample (*asterisks* indicate 'prints' of some of the missing cells), demonstrating a lack of cell adhesion between the blastomeres in these early embryos. (**C**–**D**) are different optical sections; (**F**) is a higher magnification of one of the cells shown in (**E**). Scale bars: (**A**, **C**–**E**), 100 μm; (**B**, **F**) 20 μm

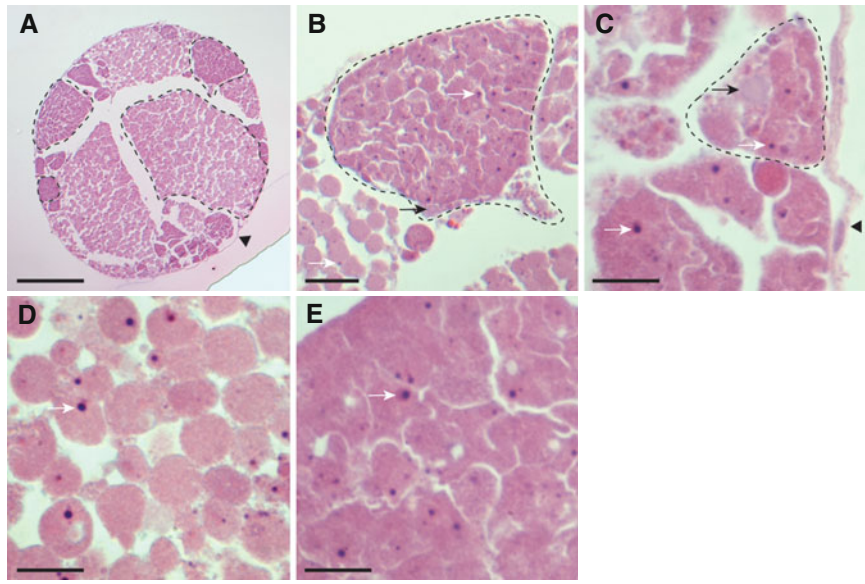

Fig. 4.8 Early cleavage in *Amphimedon queenslandica*. (**A**) Whole embryo. (**B**) Large blastomere with peripheral cytoplasm around nurse cell mass. (**C**) Smaller blastomere with more central nucleus. (**D**) *Light pink* nurse cells. (**E**) *Dark pink* nurse cells. All panels show H+E-stained median sections; *arrowhead*, maternal layer; *dashed lines*, boundary of blastomeres; *black arrows*, blastomere nuclei; *white arrows*, pyknotic nuclei of nurse cells. Scale bars: (**A**) 100 μm; (**B**) 20 μm; (**C**–**E**) 10 μm

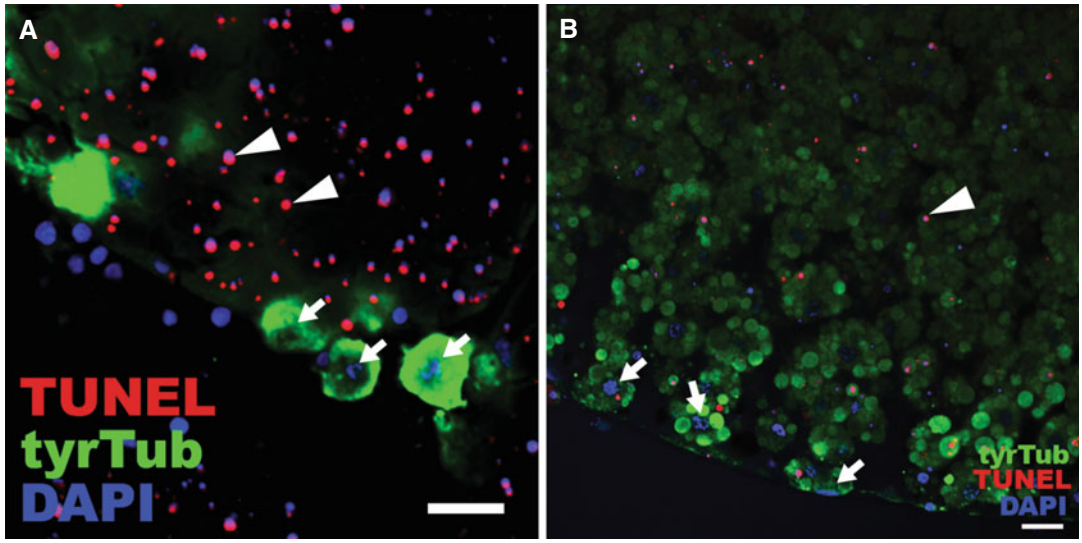

Fig. 4.9 TUNEL analysis of early *Amphimedon queenslandica* development. (**A**) Early cleavage. Note the periphery of the macromeres and the cytoplasm of the micromeres are enriched in tyrosine tubulin. (**B**) Solid blastula. Scale bars: 10 μm. Both are embryos stained with DAPI (*blue*), anti-tyrosine tubulin (*green*) and TUNEL (*red*); *arrowhead*, example TUNEL positive nuclei or nuclear fragments; *arrows*, embryonic nuclei

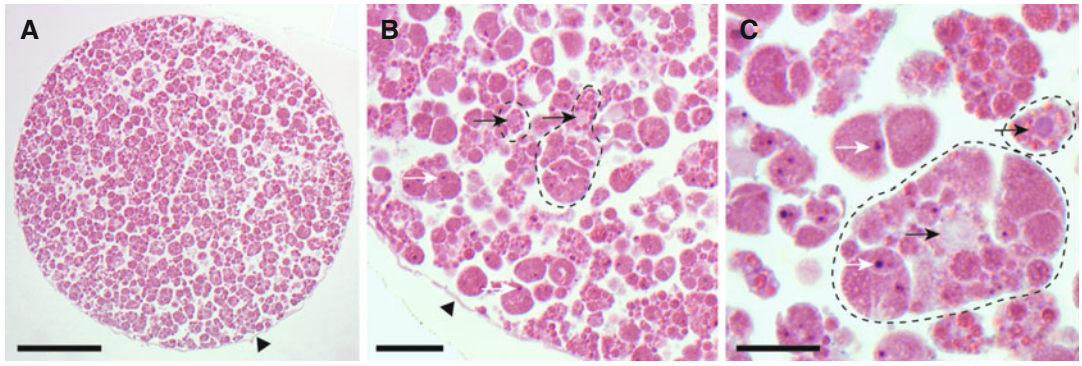

Fig. 4.10 Late cleavage in *Amphimedon queenslandica*. (**A**) Whole embryo. (**B**) Blastomeres in loose aggregation. (**C**) Variation in blastomere sizes. All panels show H+E-stained median sections; *arrowhead*, maternal layer; *dashed lines*, boundary of blastomeres; *black arrows*, blastomere nuclei; *white arrows*, pyknotic nuclei of nurse cells. Scale bars: (**A**) 100 μm; (**B**) 20 μm; (**C**) 10 μm

and loaded with yolk that appears to be derived from nutritive maternal nurse cells (e.g., Fell 1969). These large blastomeres contain large quantities of smaller eosinophilic (thus protein-rich) bodies that appear to be derived from nurse cells undergoing programmed cell death, based on the presence of compact pyknotic nuclei with intensely basophilic staining (Fig. 4.8). Terminal deoxynucleotidyl transferase dUTP nick end labeling (TUNEL) – a method that detects fragmented DNA – of pyknotic nuclei in these bodies is consistent with these being derived from apoptosing nurse cells (Fig. 4.9A).

Blastomere cytoplasm appears as a thin layer around the mass of yolk-containing vesicles, with embryonic nuclei visible at the cell periphery (Fig. 4.8, black arrows). The extent of these yolk reserves means that neither blastomere cytoplasm nor cell boundaries are always apparent (Figs. 4.7 and 4.8; Leys and Degnan 2002).

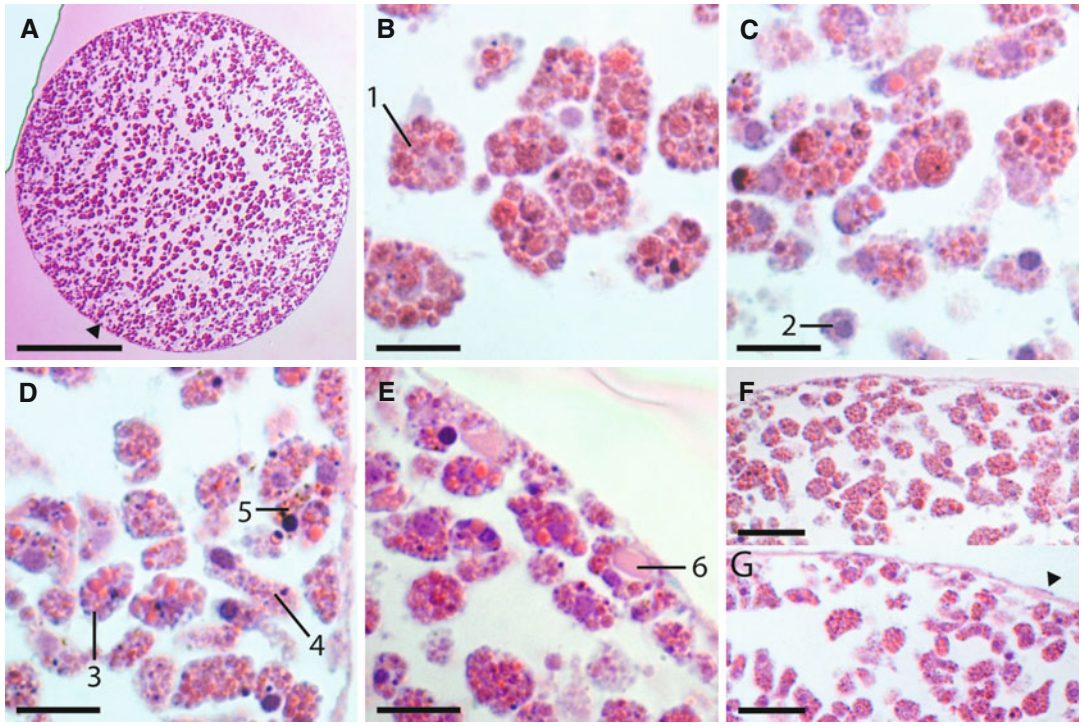

Fig. 4.11 Brown embryo stage. (**A**) Whole embryo. (**B**) Type 1, granular macromeres (‘*1*’). (**C**) Granular macromeres and micromeres (‘*2*’). (**D**) Type II, globular macromeres (‘*3*’), amoeboid cells (‘*4*’), and pigment cells (‘*5*’). (**E**) Sclerocyte (‘*6*’). (**F**, **G**), opposing sides of the embryo. All panels show H+E-stained median sections; *arrowhead*, maternal layer. Scale bars: (**A**) 100 μm; (**B**–**E**) 10 μm; (**F**–**G**) 20 μm

As cleavage progresses, the blastomeres reduce in size, and the number and concentration of pyknotic nuclei decreases (Figs. 4.9B and 4.10).

At the end of cleavage, a solid blastula forms, which is light brown in colour (Fig. 4.11). These ‘brown’ embryos contain a mixture of loosely aggregated cell types, of which six are readily identifiable: early sclerocytes around the outer margin of the embryo, two larger cell types with a variety of inclusions (designated here as type I and II macromeres), large amoeboid cells, pigment cells, and a minor micromere population (Fig. 4.11B–E). The type I and II macromeres are both spherulous and contain granular or homogenous inclusions, respectively. The amoeboid cells possess smaller and more lightly eosinophilic inclusions and larger nuclei with dense heterochromatin around their periphery. The early differentiation of some cell types, especially sclerocytes, occurs in a range of sponge embryos (Fell 1969; Maldonado and Berquist 2002; Leys 2003). Despite displaying characteristics of their final larval differentiated state (e.g., pigmentation, deposition of spicule matrix, ciliation), these cells remain to be patterned in the embryo and thus maintain the capacity to respond to positional signals and migrate appropriately.

Asymmetric Cell Division and Transcript Localisation

During cleavage an increasing number of small blastomeres are present on the periphery of the embryo and nestled between the macromeres. Following the fate of daughter cells originating from individual macromeres injected with high molecular weight tetramethylrhodamine dextran confirms that macromeres divide asymmetrically, giving rise to micromeres, typically 2–4 μm in diameter, and macromeres, initially most often >50 μm in diameter; symmetric cell divisions may occur in late cleavage (Fig. 4.12). The location of the daughter cells of individually labelled

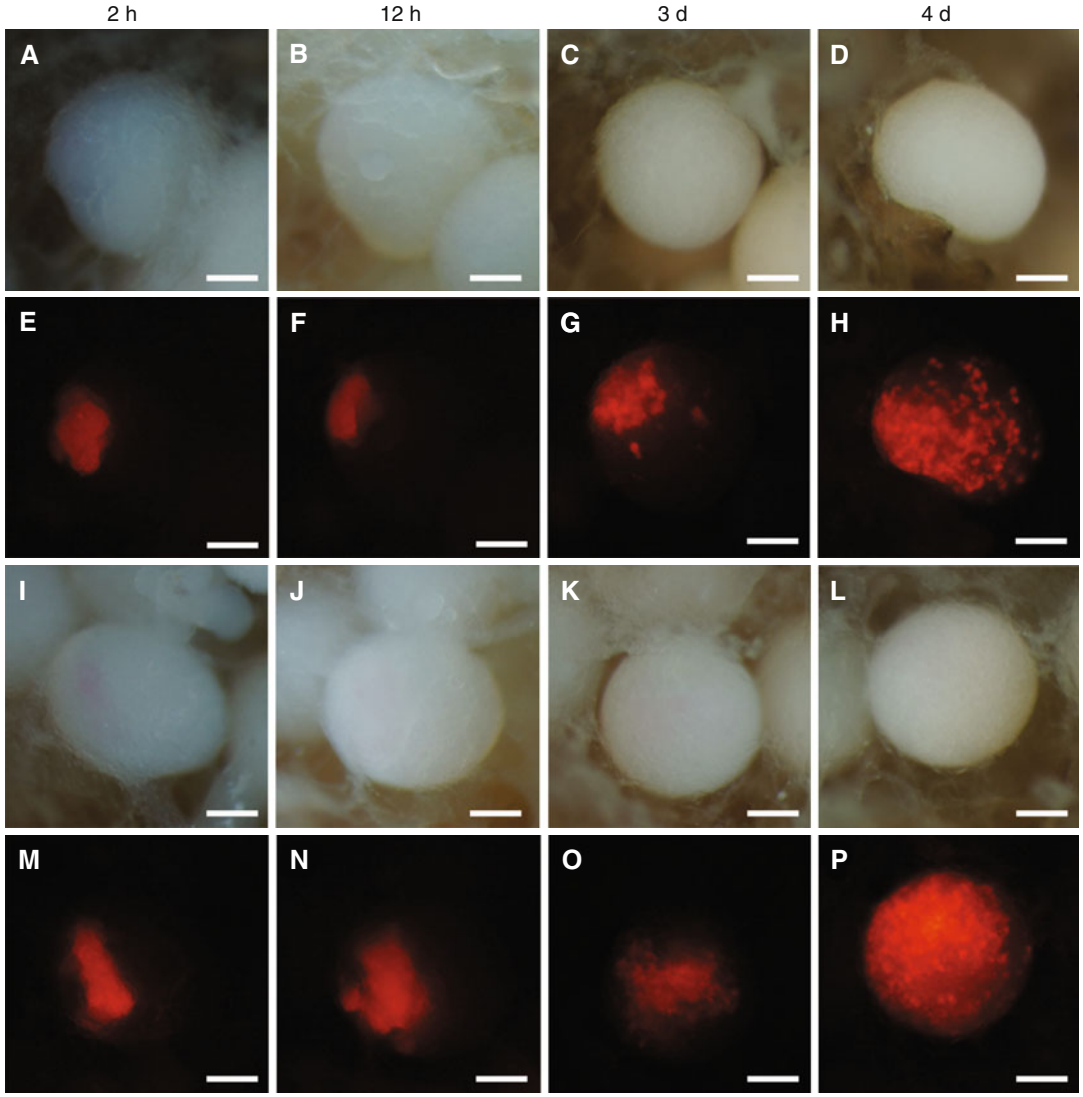

Fig. 4.12 Cell lineage analysis of randomly labelled *Amphimedon queenslandica* macromeres. Two experiments are shown (*top* (**A**–**H**) and *bottom* (**I**–**P**)). In both cases, a macromere is injected with a high molecular weight fluorescent dextran suspension, and the localisation of this fluorescent marker is traced over 4 days of development (time postinjection on *top*). Scale bars: 100 μm

macromeres provides no evidence of stereotypical or predictable cell lineages or cleavage patterns. Instead, cleavage appears to be chaotic.

Morphologically distinct pigment cells, sclerocytes, and ciliated cells are first detected during cleavage throughout the embryo (Fig. 4.11; Leys and Degnan 2002). Consistent with the early specification and determination of these cell types is the detection of transcripts encoding a number of conserved developmental transcription factors in subpopulations of micromeres at cleavage, including NK homeobox genes *Bsh* and *Tlx*, LIM homeobox gene *Lhx3/4*, and the nuclear receptor gene *NR1* (Fig. 4.13; Larroux et al. 2006, 2007; Fahey et al. 2008; Bridgham et al. 2010; Srivastava et al. 2010b).

Further analysis of *Lhx3/4* mRNA localisation at cleavage reveals transcripts are not only

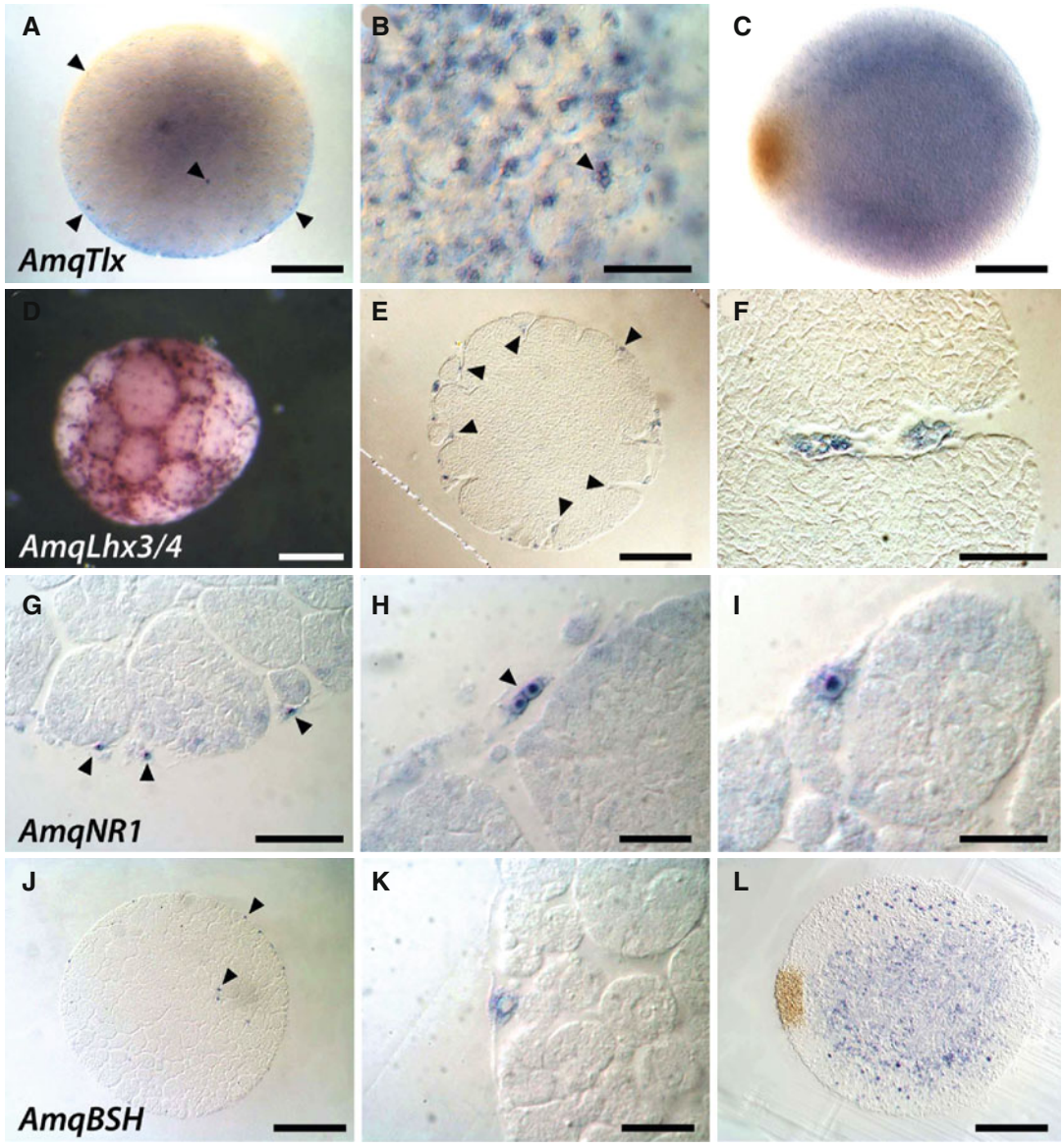

Fig. 4.13 Expression of transcription factor genes in micromeres at cleavage. (**A**–**C**) Localisation of *AmqTlx* in micromeres and sclerocytes during cleavage (**A**, **B**) and spot stage (**C**). (**D**–**F**) Localisation of *AmqLhx3/4* in micromeres during cleavage (**A**, **B**) and spot stage (**C**). (**G**–**I**) Localisation of *NR1* in micromeres during. (**J**–**L**) Localisation of *AmqBSH* in micromeres. *Arrowheads*, example cells enriched with the transcript. (**A**, **B**, **C**, **H**, **I**, **J**, **K**, and **L**), sections; (**D**, **E**, **F**, **G**), whole mounts. Scale bars: (**A**, **C**, **D**, **F**, **G**, **H**), 100 μm; (**B**, **I**, **K**, **L**), 10 μm; (**E**, **I**), 25 μm **L** (From Larroux et al. 2006)

present in individual micromeres but are also associated with the cortex of adjacent macromeres (Fig. 4.14). Macromere cortices and micromeres are enriched in microtubules (Fig. 4.15). Nuclei also localise to the macromere cortical region, consistent with these being regions of cell division. Asymmetric inheritance of cell fate determinants, in the form of localised mRNAs, is widespread in animal development (reviewed in Knoblich 2010; Medioni et al. 2012). This typically requires the localisation of particular mRNAs via cytoskeleton-mediated

active transport to a defined cortical region of the cell. These results suggest that such a mechanism is operational during *Amphimedon queenslandica* cleavage and probably essential for the early specification and determination of micromere fate.

A more extensive survey of gene expression patterns in cleaving embryos indicates

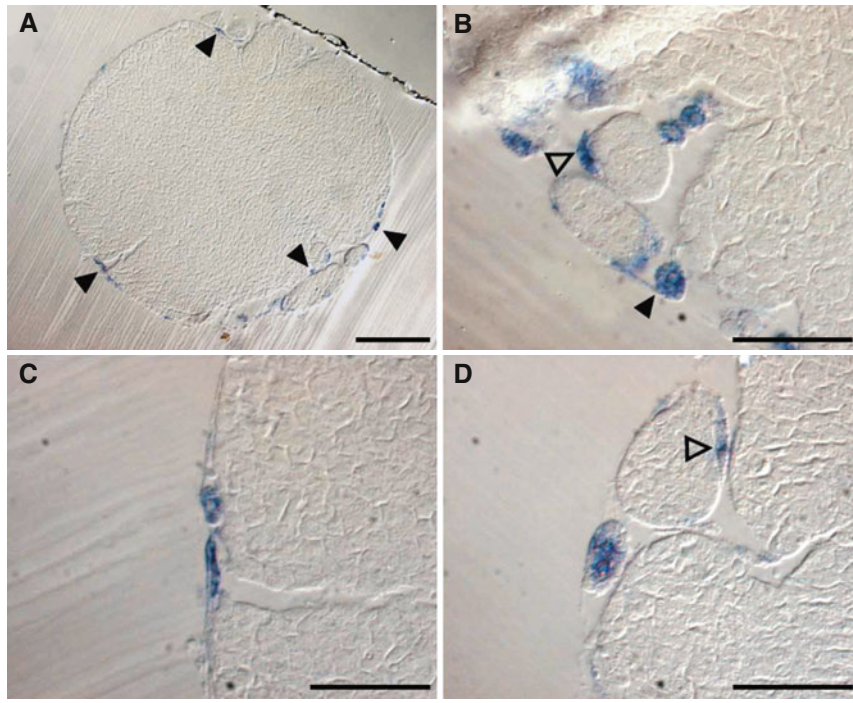

Fig. 4.14 Localisation of *AmqLhx3/4* mRNA in macromeres and micromeres. (**A**) Cleaving embryo, low magnification. (**B**–**D**) Higher magnification of cortex and micromeres. *Arrowheads*, example cells and cortical regions enriched with the transcript. Scale bars: (**A**) 100 μm; (**B**–**D**) 10 μm

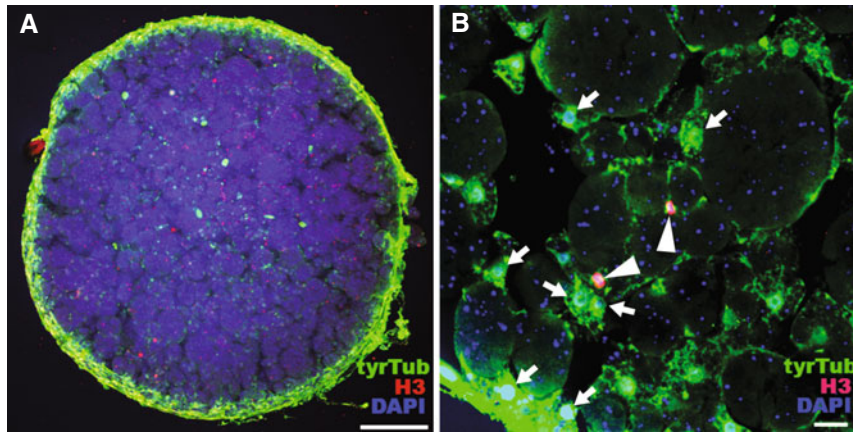

Fig. 4.15 Localisation of microtubules and mitotic figures to macromere cortices. (**A**) Cleaving embryo showing mitotic cell nuclei (*red*). (**B**) Higher magnification showing dividing nuclei are localised to macromere cortices, which are also enriched in microtubules. *Arrowheads*, phosphorylated histone 3 (H3) positive nuclei (*red*); *arrows*, example micromere nuclei (*blue*); anti-tyrosine tubulin immunoreactivity (*green*). Scale bars: (**A**) 100 μm; (**B**) 10 μm

that the localisation of transcripts to subsets of micromeres is widespread in *Amphimedon queenslandica* (Fig. 4.16). The lack of similarity in many of the in situ hybridisation patterns is consistent with different transcripts being localised to different sets of micromeres; this suggests that cell fate specification and determination starts early in *A. queenslandica* embryogenesis. This mode of cell specification may be an important feature of the early development of many sponges with similar external embryological characteristics (cf. Ereskovsky 2010).

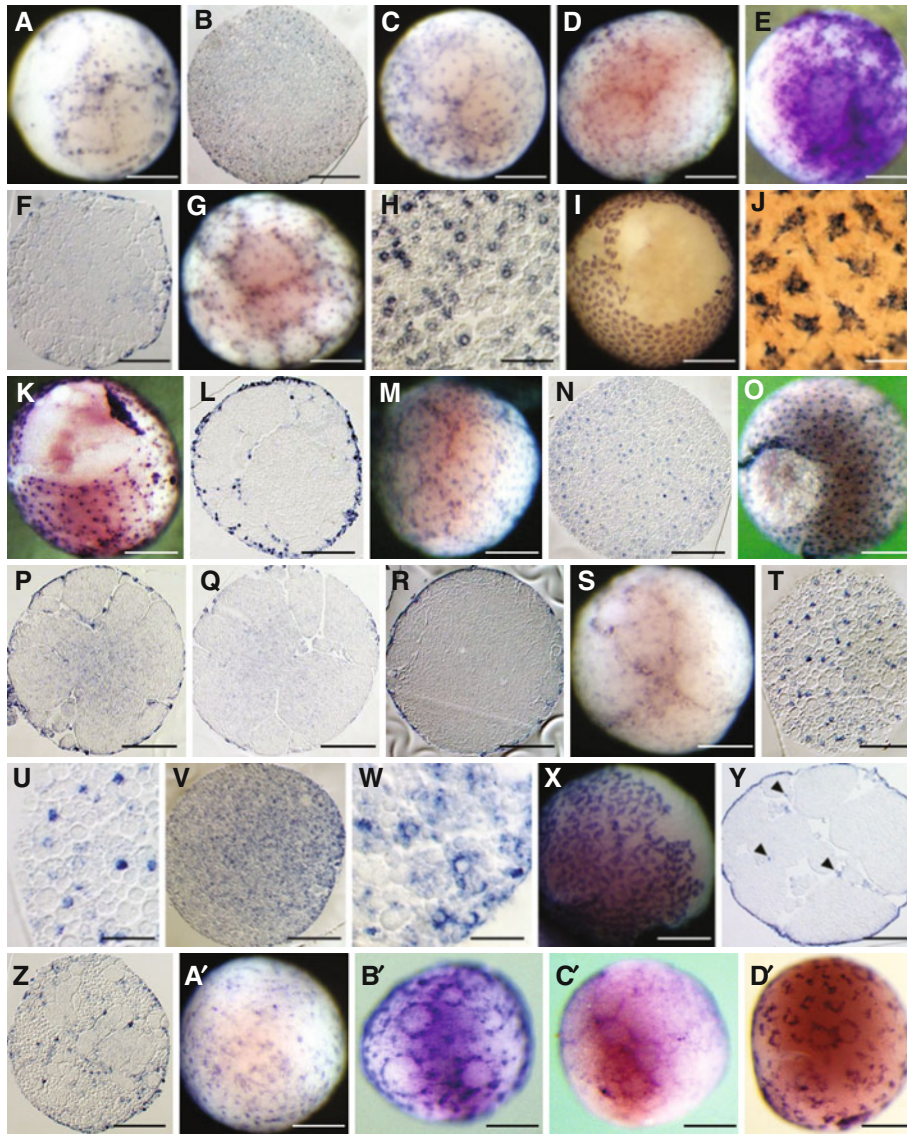

Fig. 4.16 Examples of localised transcripts in cleaving *Amphimedon queenslandica* embryos. (**A**) *AmqWntA*. (**B**) *AmqWntB*. (**C**) *AmqTGF-β*. (**D**) *AmqFzdA*. (**E**, **F**) *AmqFzdB*. (**G**, **H**) *Amqβ-catenin*. (**I**, **J**) *AmqSFRPD* in maternal follicle cell layer. (**K**, **L**) *AmqAxin* predominantly in external micromeres but also a smaller number of internal micromeres. (**M**) *AmqDsh*. (**N**) *Amq-Gro*. (**O**) *Amq-Lrp5/6* in maternal follicle cell layer. (**P**) *AmqGSK*. (**Q**) *AmqAPC*. (**R**) *AmqTcf*. (**S**) *AmqHedgling*. (**T**, **U**) *AmqPellino*. (**V**, **W**) *AmqMyD88*. (**X**, **Y**) *AmqSTmyhc* in maternal follicle cell layer and few internal micromeres. (**Z**) *AmqTollip*. (**A′**) *AmqCry1*. (**B′**) *PL10*. (**C′**) *Nanos*. (**D′**) *Vasa*. Scale bars: (**A–G**, **I**, **K–T**, **V**, **Y–D′**), 100 μm; (**H**, **U**, **W**), 25 μm; (**J**), 10 μm. (**A–R**) (From Adamska et al. 2010); (**T–W** and **Z**) (From Gauthier et al. 2010); (**X** and **Y**) (From Steinmetz et al. 2012); (**A′**) (From Rivera et al. 2012)

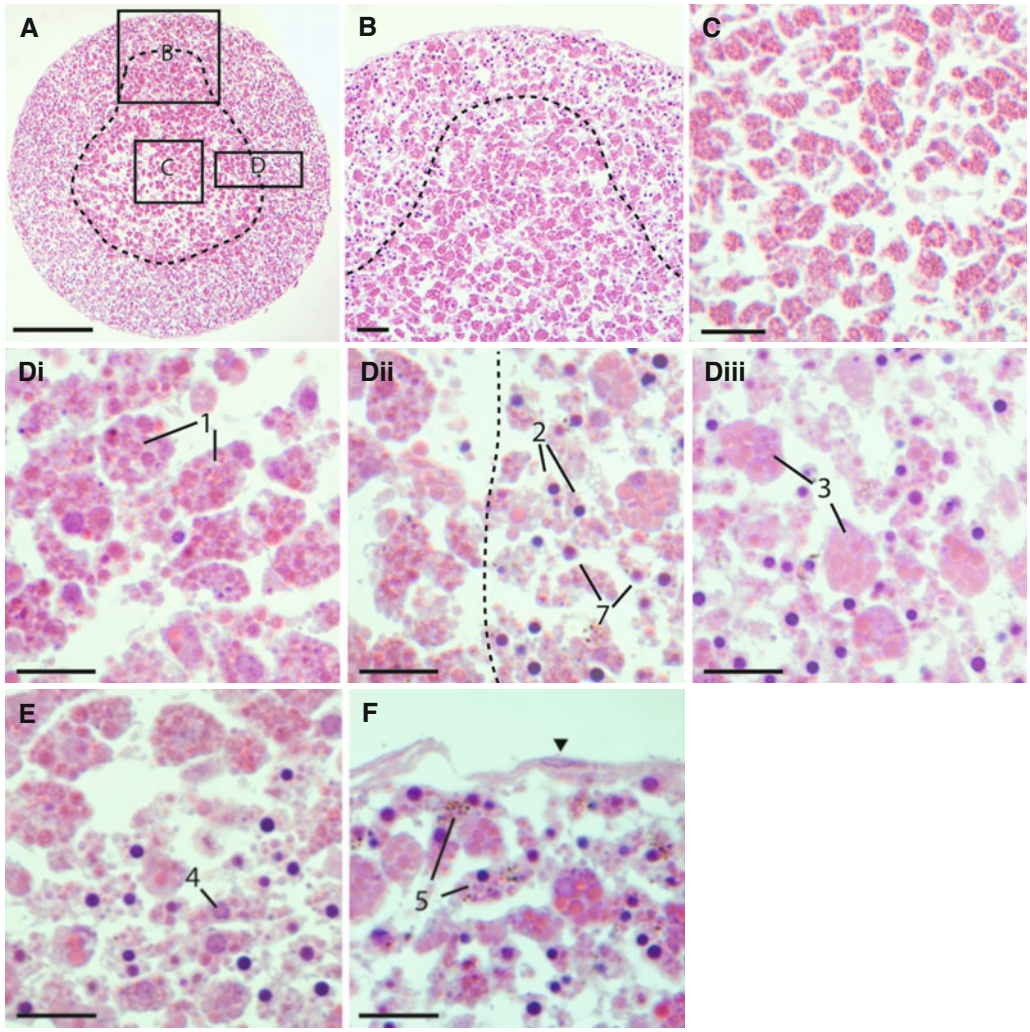

Fig. 4.17 Cloud stage embryos. (**A**) Whole embryo. (**B**) Posterior pole and underlying macromeres. (**C**) Inner layer. (**D**) Progression from inner (*i*) to outer (*iii*) layer showing locations of type 1 granular macromeres (‘*1*’), type 1 micromeres (‘*2*’), type II globular macromeres (‘*3*’), and type II micromeres (‘*7*’). (**E**) Amoeboid cells in the outer layer (‘*4*’). (**F**) Pigment cells towards the posterior pole (‘*5*’). All panels show H+E-stained median sections; *dashed line*, inner/outer cell layer boundary; *arrowhead*, maternal layer. Scale bars: (**A**), 100 μm; (**B**–**C**), 20 μm; (**D**–**F**), 10 μm

In addition to various transcription factor mRNAs, transcripts that localise to micromeres at cleavage include those encoding components of conserved signalling pathways, innate immunity factors, structural proteins, and RNA-binding proteins and presumptive germ line factors. It is worth noting that the last group, which includes *vasa*, *nanos*, and *PL10*, displays transcript enrichment around a subset of micromeres (Fig. 4.16B′–D′).

Cell Layer Formation and Establishment of Axial Polarity

Cleavage is followed by a period of differential cell movement that sorts these different cell types into inner and outer layers (Fig. 4.6C, D), with ciliated cells, sclerocytes, and pigment cells being enriched in the outer portion of the embryo (Figs. 4.11 and 4.17; Leys and Degnan 2002). The inner cell mass (ICM) is primarily composed

of large granular cells (Fig. 4.17). At this stage, cells appear mesenchyme-like, lacking robust cell junctions and being surrounded by a collagenous extracellular matrix (ECM) (Leys and Degnan 2002). After this initial sorting, cells continue migrating to become patterned along the anterior-posterior (AP) axis (Fig. 4.1; Leys and Degnan 2002; Degnan et al. 2005; Adamska et al. 2007a, 2010).

Tracing cells on the surface of embryos, by labelling with the fluorescent lipophilic dye DiI, confirms that early *Amphimedon queenslandica* embryos undergo extensive cellular rearrangements between late cleavage (brown stage) and the establishment of the AP axis ('cloud' and 'spot' stages) (Fig. 4.18; Adamska et al. 2010). Accordingly, the spacing between cells in cleavage and early brown stages probably reflects a lack of robust intercellular adhesion as well as a lack of extensive extracellular material. A similar event has been inferred to occur in embryos of *Ephydatia* prior to the differentiation of cell layers (De Vos et al. 1991). These broad cell movements represent morphogenesis via 'differential centrifugal migration' or 'multipolar migration/delamination' and commonly rely on cell sorting via the relative adhesive properties of each cell type (Leys and Ereskovsky 2006).

Just before the cloud stage, *Amphimedon queenslandica* embryos undergo compaction (Adamska et al. 2010), which may mark the culmination of the mass cell migratory events. This also coincides with stronger cell adhesion in the embryo and the increased density of ECM (Leys and Degnan 2002; Adamska et al. 2010). The increased density of cells and the appearance of ECM in the inner layer of the cloud stage (Fig. 4.17; Leys and Degnan 2002) support this timing and interpretation of events. External cells labelled with DiI at the cloud stage and later in development do not migrate to the same extent as cells labelled during cleavage and brown stages (Fig. 4.18), suggesting that the majority of the cells in the outer layer of the embryo reach their final embryonic territory by the end of the cloud stage (i.e., spot stage).

Localisation of Wnt and TGF-β Transcripts in the Early Embryo

The establishment of the bilayered embryo with AP axial polarity is preceded by the localisation of *Wnt*-expressing cells in the future posterior half of the embryo (Adamska et al. 2007a, 2010). These cells initially appear to be evenly distributed in the cleaving embryo and then appear to migrate posteriorly (Fig. 4.19). The mechanisms underlying the coalescing of these *Wnt-expressing* cells towards the future posterior side of the embryo remain unknown. It is yet to be determined if the Wnt pathway or another mechanism, such as signalling from the maternal follicle layer, directs the formation of the embryonic axis. Nonetheless, many of the components of the Wnt pathway also are expressed in cleaving embryos, usually in subsets of micromeres, or the surrounding follicle layer (Fig. 4.16; Adamska et al. 2007a, 2010), suggesting that some embryonic cells are competent to respond to the Wnt ligand.

A gene encoding a TGF-β ligand is expressed initially in a fraction of small cells distributed throughout the outer layer of the cleaving *Amphimedon queenslandica* embryo (Adamska et al. 2007a). During the formation of the bilayered embryo, transcripts become differentially localised along the AP axis and enriched at the poles (Fig. 4.19). These results are consistent with Wnt and TGF-β pathways working together to pattern the embryonic AP axis, from which will form the radially symmetrical *A. queenslandica* larva. During the formation of the cell layers and the establishment of the primary (AP) axis, many genes are differentially expressed in the inner and outer cell layers (Fig. 4.20).

In most eumetazoans, Wnt and TGF-β pathways are responsible for patterning of the AP and dorsoventral body axes (reviewed in Martindale 2005; see also Hayward et al. 2002; Matus et al. 2006). The differential expression of Wnt and TGF-β along the demosponge AP axis suggests that these genes were used to pattern the body plans of the first (radially symmetrical) animals (Adamska et al. 2007a, 2010).

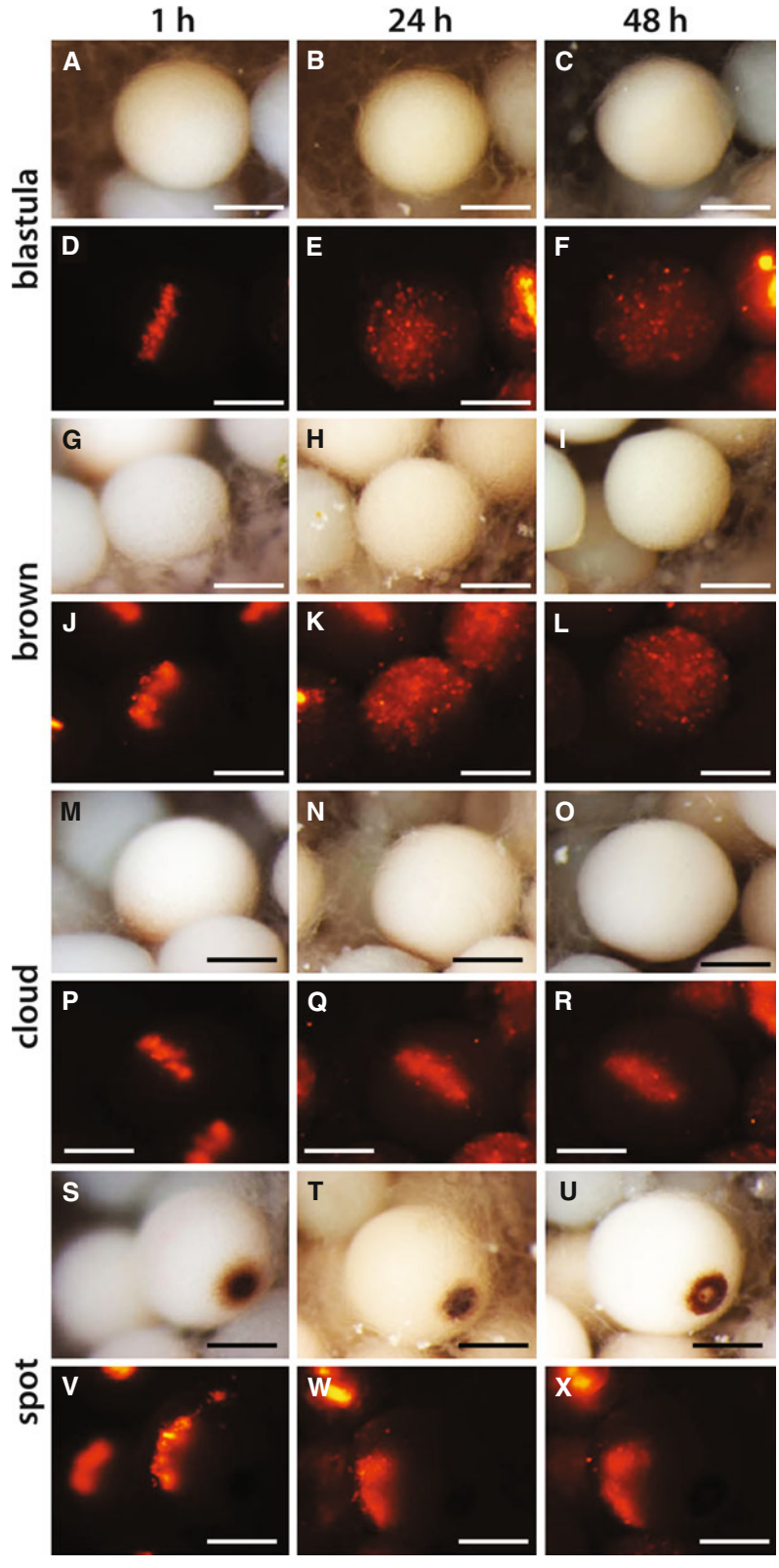

Fig. 4.18 Cell movement in *Amphimedon queenslandica* embryos. Embryos within brood chambers were 'tattooed' with a fluorescent lipophilic tracer, DiI, and photographed 1, 24, and 48 h after labelling. Embryos at four stages were labelled. (**A**–**F**) Blastula. (**G**–**L**) Brown stage. (**M**–**R**) Cloud stage. (**S**–**X**) Spot stage. *Top* panels (**A**–**C**, **G**–**I**, **M**–**O**, **S**–**U**): bright light images of the embryos; *bottom* panels (**D**–**F**, **I**–**L**, **P**–**R**, **V**–**X**): fluorescence images of the same embryos. Developmental stages are indicated to the *left*. Scale bars: 250 μm

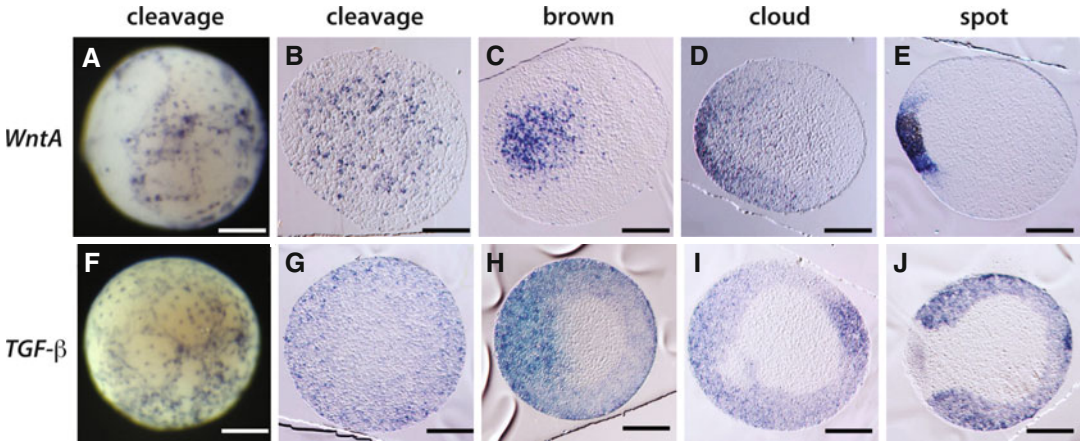

Fig. 4.19 *Wnt* and *TGF-β* expression in *Amphimedon queenslandica* early embryos. (**A**–**E**) *WntA* in situ hybridisations. (**F**–**J**) *TGF-β* in situ hybridisations, except (**H**), which is a double in situ hybridisation with *WntA* in *light blue* and *TGF-β* in *purple*. (**A**, **F**) Whole mounts. (**B**–**E**, **G**–**J**) Sections with posterior to the left. Scale bars: 100 μm (Modified from Adamska et al. (2007a) and (2010))

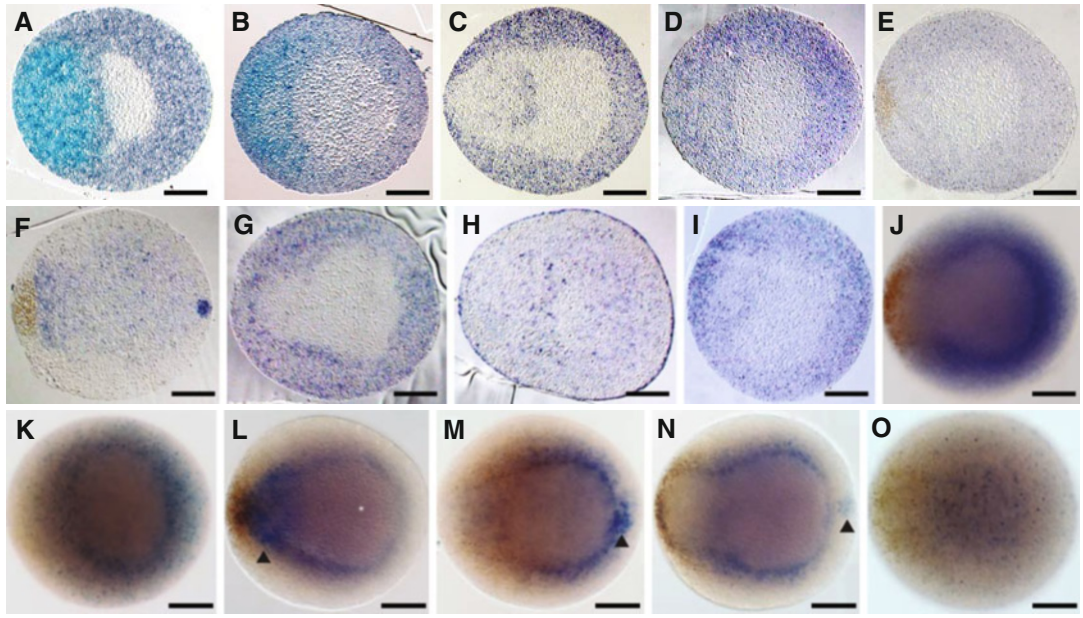

Fig. 4.20 Examples of differential gene expression of Wnt and Notch pathway components during cell layer and posterior spot formation. Posterior to the left in all micrographs. (**A**–**I**) Wnt pathway components (sections). (**J**–**O**) *Notch* and *Delta* (whole mounts) (**A**) *FzdA*. Double in situ hybridisation with *WntA* (*light blue*). (**B**) *β-catenin*. Double in situ hybridisation with *WntA* (*light blue*). (**C**) *Gsk*. (**D**) *Dvl*. (**E**) *Gro*. (**F**) *FzdB*. (**G**) *LRP4/6*. (**H**) *TCF*. (**I**) *APC*. (**J**) *Notch*. (**K**) *Delta1*. (**L**) *Delta2*. *Arrowhead* points to expression under the forming pigment spot. (**M**) *Delta3*. *Arrowhead* points to expression in a group of cells located towards the anterior of the embryo. (**N**) *Delta4*. *Arrowhead* points to expression in a group of cells located towards the anterior of the embryo. (**O**) *Delta5*. Scale bars: 100 μm. (**A**–**J**) are (From Adamska et al. 2010); (**J**–**O**) are (From Richards and Degnan 2012)

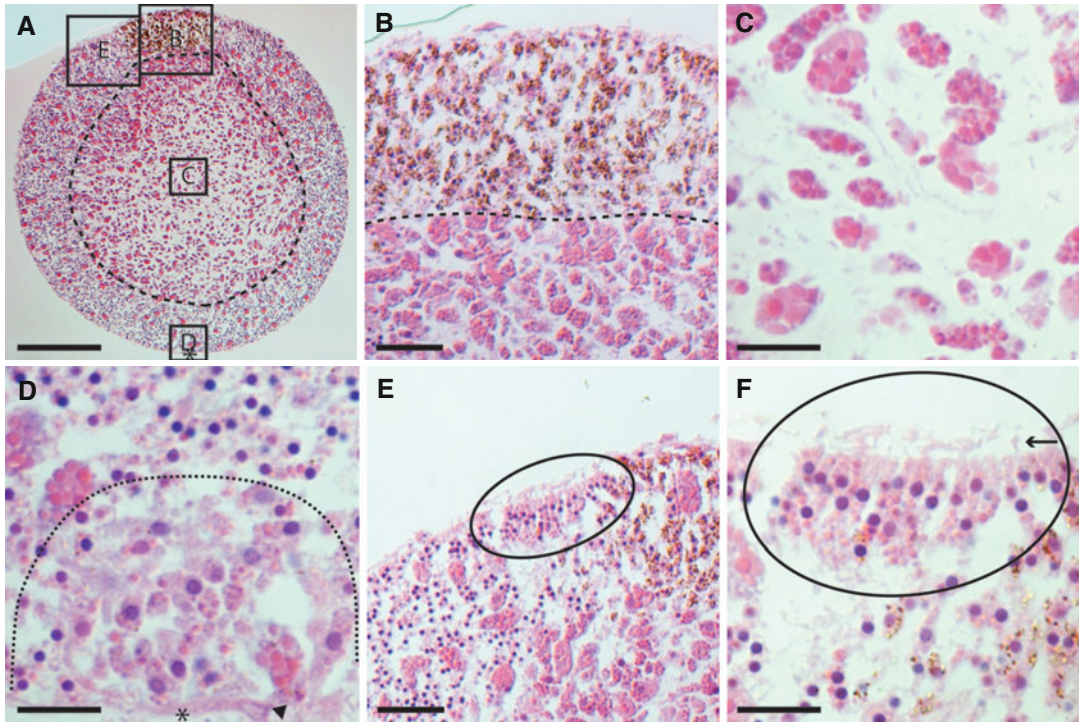

Fig. 4.21 Early spot stage embryos. (**A**) Whole embryo. (**B**) Pigment spot. (**C**) Inner layer. (**D**) Anterior pole cells (*dotted line*). (**E**) Posterior ciliated cells (*oval*). (**F**) Higher magnification of (**E**). All panels show H+E-stained median sections; *dashed line*, inner/outer cell layer boundary; *asterisk*, anterior pole; *arrowhead*, maternal layer; *arrow*, cilia. Scale bars: (**A**), 100 μm; (**B**, **E**), 20 μm; (**C**–**D**, **F**), 10 μm

LATE EMBRYONIC DEVELOPMENT IN *AMPHIMEDON QUEENSLANDICA*

In *Amphimedon queenslandica*, late embryonic development is considered to start at the spot stage, when the bi-layered embryo has an obvious AP axis and when the larval body plan is completely formed. In some cases, cells combine with other cells of the same type to form simple tissues, including the ciliated epithelium, the anterior cuboidal cell cluster, the pigment ring, and the ciliated ring. The latter two tissues combine to form a functional photosensory organ (Rivera et al. 2012).

Spot Stage and Commencement of Larval Tissue Formation

The early spot stage is characterised by the coalescence of the pigment cells at the posterior pole (Fig. 4.21A, B). Directly beneath the pigment spot, a dense group of type I macromeres remains, as seen in earlier stages, and the inner layer contains an increasing amount of extracellular material (Fig. 4.21C). The cell population at the anterior pole has formed a compact group (Fig. 4.21D). At the posterior, a group of columnar cells with an apical cilium and basal inclusions are aligned adjacent to the pigment spot (Fig. 4.21E, F).

In later spot stage embryos (Fig. 4.22A), a population of micromeres (non-pigmented) at the posterior pole becomes apparent; these form a ‘cap’ in the centre of the pigment spot (Fig. 4.22B). Directly opposite, the group of cells at the anterior pole is more condensed than previously (Fig. 4.22C). The outer epithelium of the embryo forms in a posterior to anterior progression (Fig. 4.22D), and the follicle layer separates from the embryo as the outer epithelium gains integrity (white arrows, Fig. 4.22D). Immediately

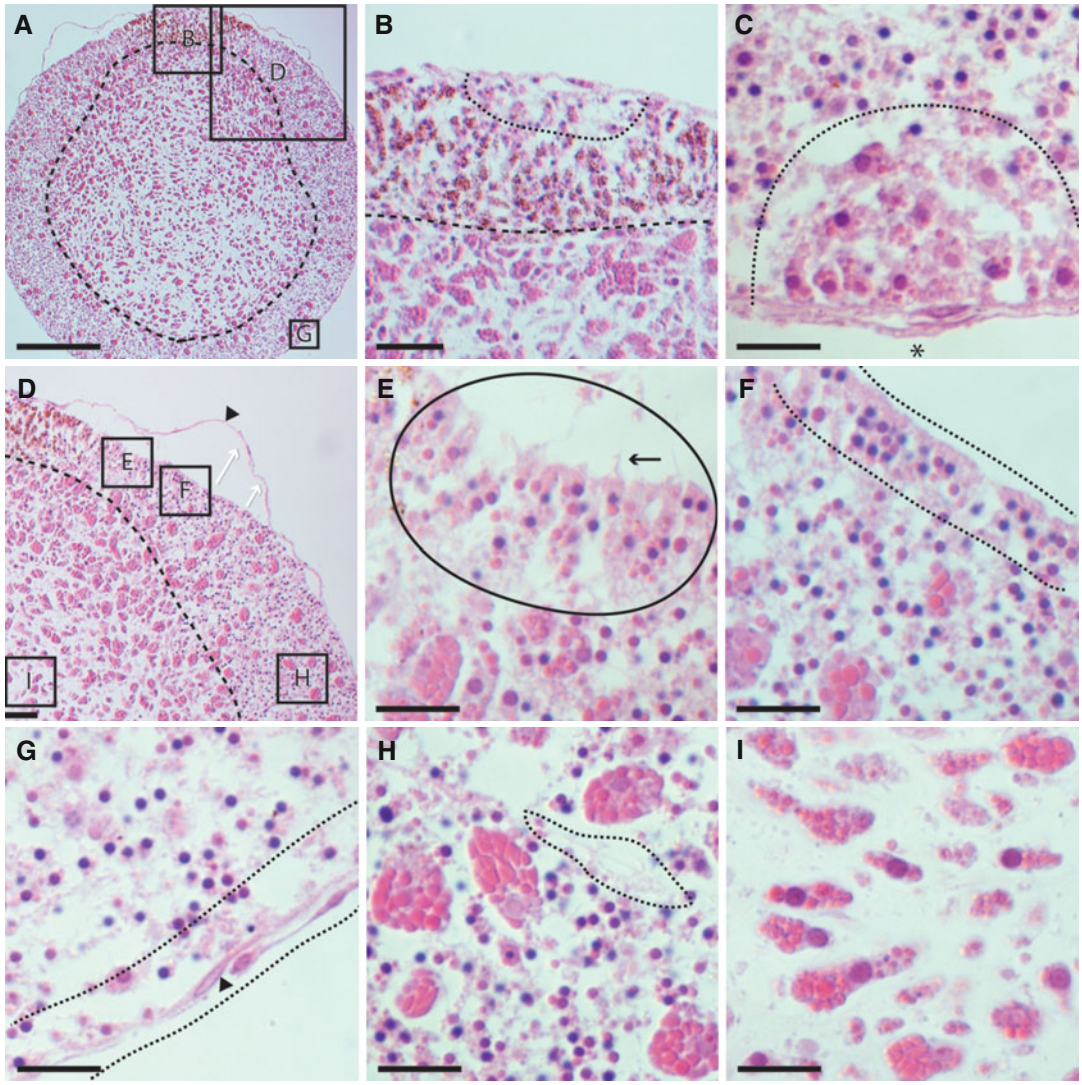

Fig. 4.22 Late spot stage embryos. (**A**) Whole embryo. (**B**) Pigment spot with small cap of non-pigmented cells (*dotted line*). (**C**) Anterior pole cells (*dotted line*). (**D**) Separation of maternal layer (*white arrows*). (**E**) Posterior ciliated cells (*oval*). (**F**) Forming border of posterior epithelium (*dotted lines*). (**G**) Unformed border of anterior outer layer (*dotted line*). (**H**) Outer layer with sclerocyte (*dotted lines*). (**I**) Inner layer cells and extracellular matrix. All panels show H+E-stained median sections; *dashed line*, inner/outer cell layer boundary; *asterisk*, anterior pole; *arrowhead*, maternal layer; *black arrow*; cilia. Scale bars: (**A**), 100 µm; (**B**, **D**) 20 µm; (**C**, **E**–**J**), 10 µm

adjacent to and anterior of the pigment spot is a population of ciliated epithelial cells (Fig. 4.22E). Immediately anterior to these, micromeres of the outer layer are lined up along the margin of the embryo and are thickened apically, forming a distinct boundary edge (Fig. 4.22F). Closer to the anterior pole, the micromeres of the outer layer are not organised into a distinct layer (Fig. 4.22G).

Pigment Ring Formation

The ring stage is identified by the wrinkled appearance of the embryo and the transformation of the pigment spot into a pigment ring at the posterior pole (Fig. 4.23A). Ring formation occurs via an increase in the non-pigmented cells found at the posterior pole and the migration of pigment

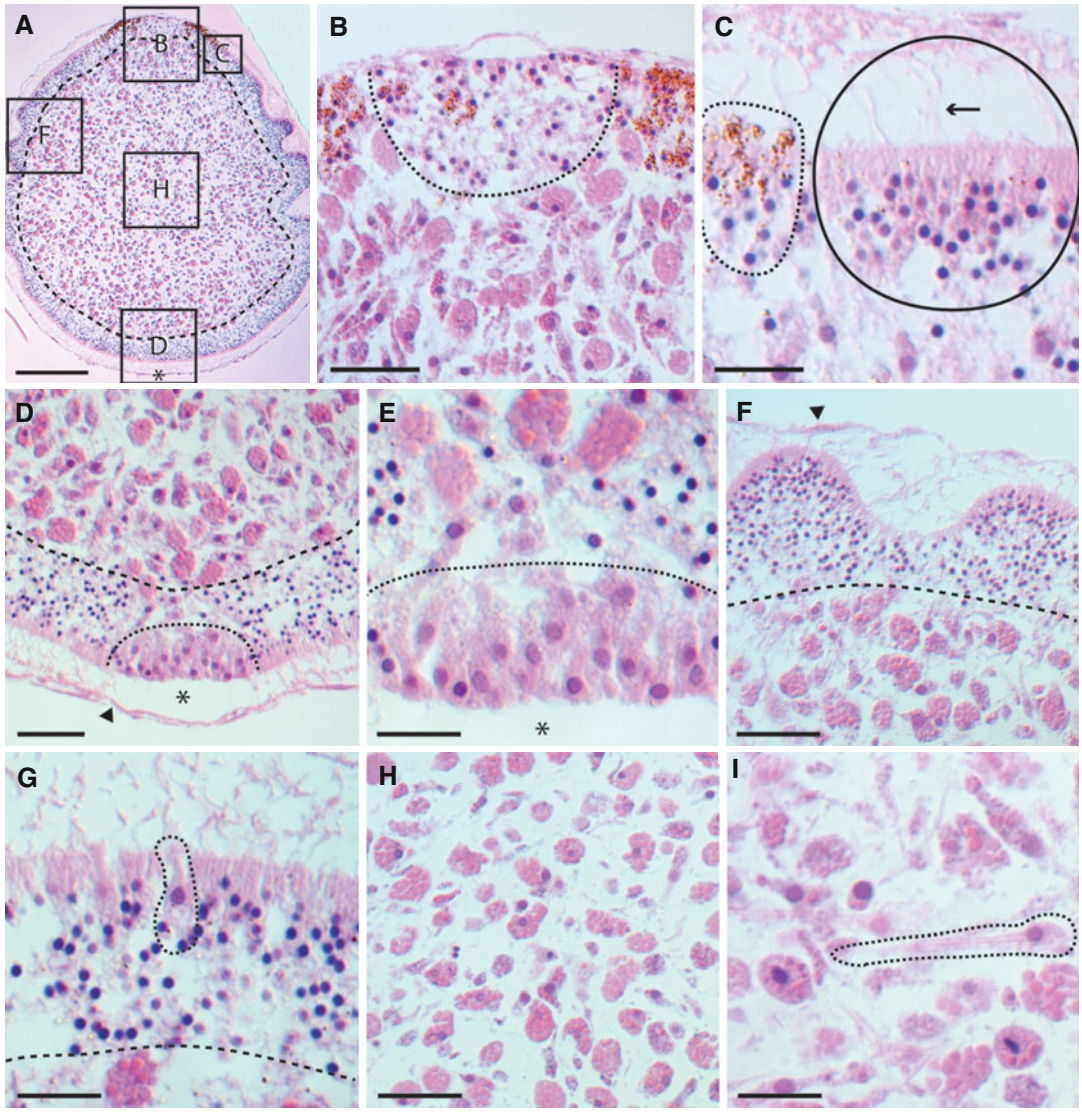

Fig. 4.23 Early ring stage embryos. (**A**) Whole embryo. (**B**) Posterior pole, non-pigmented cells (*dotted line*). (**C**) Posterior ciliated cells (*oval*) and pigment cells (*dotted line*). (**D**) Anterior pole cells (*dotted line*). (**E**) Higher magnification of (**D**). (**F**) Wrinkled outer epithelium. (**G**) Flask cell (*dotted line*). (**H**) Inner layer cells and extracellular matrix. (**I**) Inner layer sclerocyte (*dotted line*). (**E**, **G**, and **I**) are higher magnification images from the same regions as (**D**, **F**, and **H**), respectively. All panels show H+E-stained median sections; *Dashed line*, inner/outer cell layer boundary; *arrowhead*, maternal layer; *asterisk*, anterior pole; *arrow*, cilia. Scale bars: (**A**), 100 μm; (**B**, **D**, **F**, **H**), 20 μm; (**C**, **E**, **G**, **I**), 10 μm

cells from a central position at the posterior pole, to being more laterally located at the surface (Fig. 4.23B). In addition, the pigment cells are polarised, with the pigment granules located apically, and the nucleus assuming a basal position in each cell (Fig. 4.23C). Adjacent to the pigment cells, the posterior ciliated cells remain a distinct group, packed in a tight cluster to the exclusion of other cells in the outer layer (Fig. 4.23C). The cells at the anterior pole by now are organised into a single layer, with the nucleus assuming a more apical position in each cell (Fig. 4.23D, E).

The outer layer of the embryo is ciliated (except at the anterior and posterior poles), and, as a consequence, the follicle layer is no longer closely associated with the embryonic surface

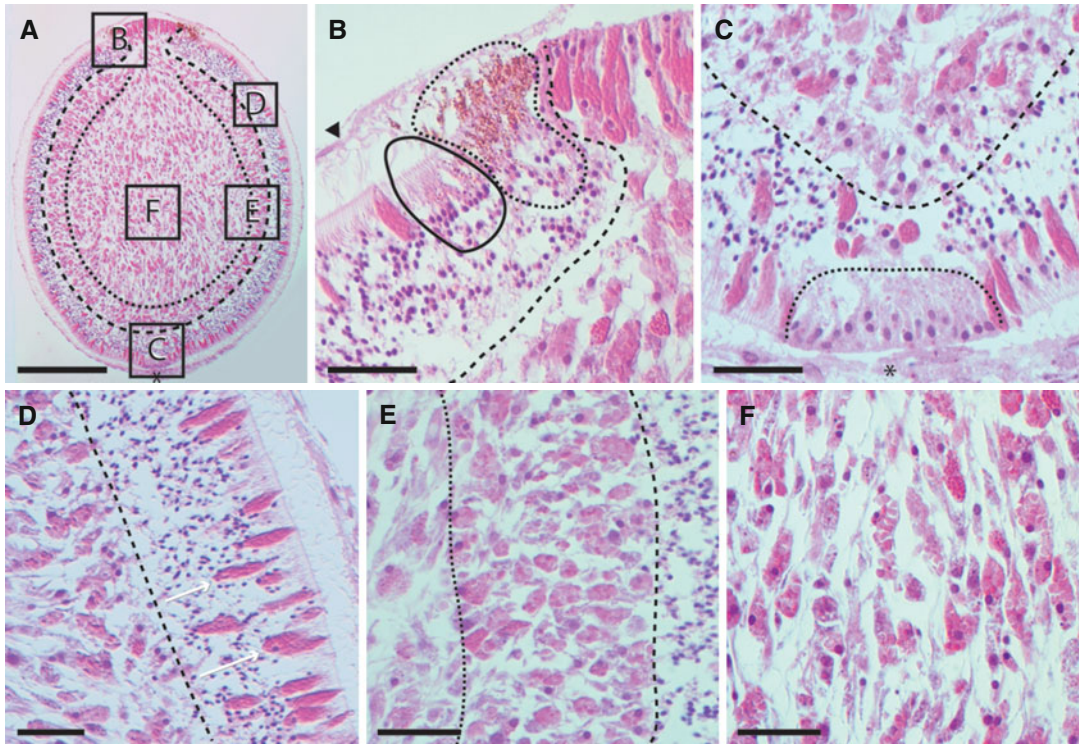

Fig. 4.24 Late ring stage embryos. (**A**) Whole embryo. (**B**) Cells of the pigment ring (*dotted line*) and associated posterior ciliated cells (*solid line*). (**C**) Anterior pole cells (*dotted line*). (**D**) Migration of globular cells (*white arrows*). (**E**) Middle layer, boundary with inner cell mass (*dotted line*). (**F**) Inner cell mass. All panels show H+E-stained median sections; *dashed line*, inner/mid cell layer boundary; *arrowhead*, maternal layer; *asterisk*, anterior pole. Scale bars: (**A**), 100 µm; (**B–F**), 20 µm

(e.g., Fig. 4.23D). The ciliated cells of the outer layer are polarised, with nuclei located basally and the apical region of each cell bearing a cilium (Fig. 4.23F, G). All macromeres have left the outer layer by this stage and are either located in the inner cell mass or at the boundary between the inner and outer layers (Fig. 4.23F). A new cell type – the flask cell (Leys and Degnan 2001) – is now identifiable amongst the ciliated epithelial cells towards the anterior of the embryo; they are ciliated with a centrally located nucleus and numerous small basally located vesicles (Fig. 4.23G). The inner layer of the embryo contains a diversity of unidentified cell types that are embedded in extracellular material (Fig. 4.23H). Numerous sclerocytes are also present (Fig. 4.23I).

The late ring embryo is elongated in comparison to earlier stages and is morphologically very similar to the larval form (Fig. 4.24A). At the posterior, the pigment cells are organised into a symmetrical ring around the pole with the apical region of each pigment cell protruding from the embryo (Fig. 4.24B). The posterior ciliated cells that lie adjacent to the pigment ring are also polarised, with basal nuclei, and the cells now appear to be clustered into small groups (Fig. 4.24B).

At the anterior pole, the cells are organised into a single layer and, in contrast to the surrounding epithelium, are non-ciliated (Fig. 4.24C). In the outer layer, which had previously been empty of macromeres, a population of globular cells (putatively derived from the type II macromere population) is now evident. These cells appear to migrate outwards from the forming subepithelial layer, through the outer layer to the periphery of the embryo (white arrows, Fig. 4.24D). A further group of globular macromeres is found at the posterior pole, within the ring of pigment cells (Fig. 4.24B). Between the ICM and the outer

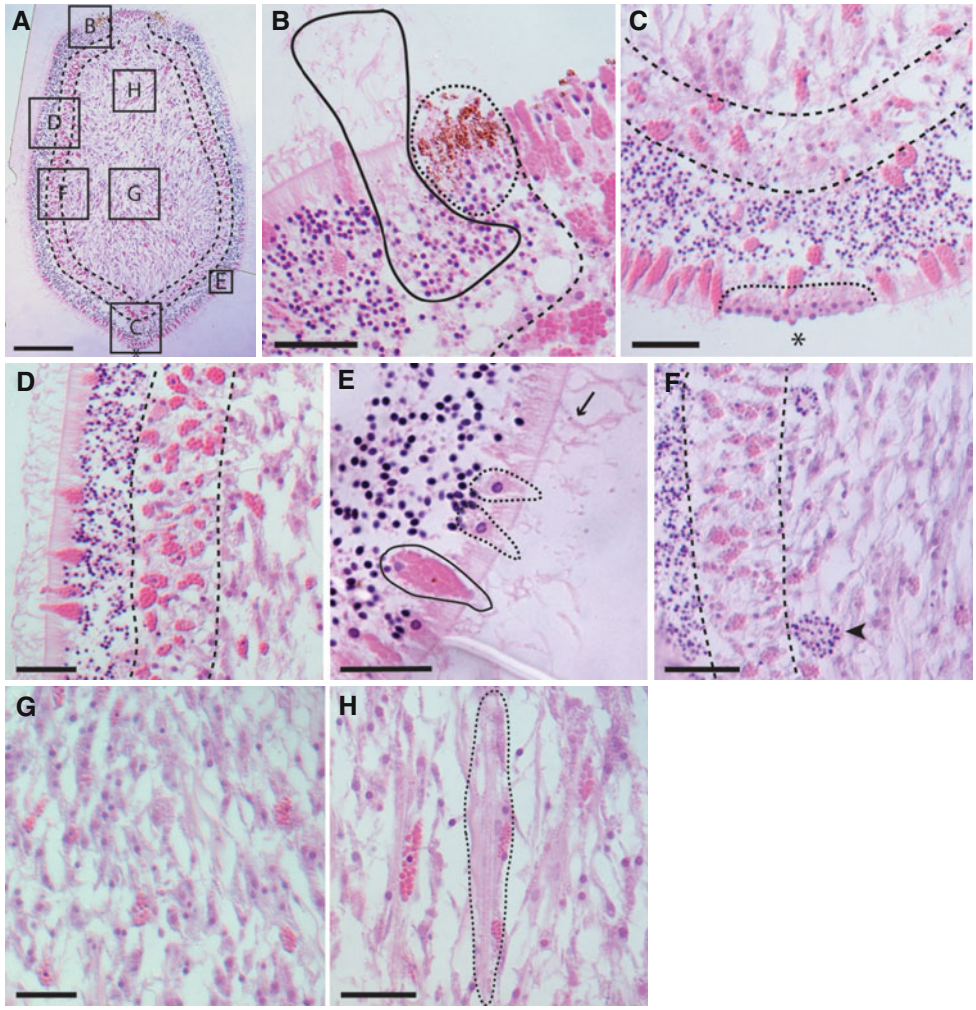

Fig. 4.25 The *Amphimedon queenslandica* larva. (**A**) Whole larva. (**B**) Cells of the pigment ring (*dotted line*) and associated posterior ciliated cells (*solid line*). (**C**) Anterior pole cells (*dotted line*). (**d**) Larval cell layers. (**E**) Intraepithelial cells: flask cells (*dotted line*) and globular cells (*solid line*). (**F**) Precocious choanocyte chambers (*arrowhead*). (**G**) Inner cell mass. (**H**) Sclerocyte bundle (*dotted line*). All panels show H+E-stained median sections; *dashed line*, cell layer boundaries; *asterisk*, anterior pole; *black arrow*, cilia. Scale bars: (**A**), 100 μm; (**B–D**, **F–H**), 20 μm; (**E**), 10 μm

epithelium, a third cell layer – the subepithelial layer – is now evident; it is composed of spherulous cells interspersed with a number of smaller, unidentified cells (Fig. 4.24E). Cells of the ICM are positioned with their long axes aligned to the anterior-posterior axis of the embryo (Fig. 4.24F). The majority of sclerocytes are now located either within the ICM or at the boundary between the ICM and the subepithelial layer (not shown).

At this late stage, some cells combine with other cells of the same type to form simple tissues, including ciliated epithelium, anterior cuboidal cells, pigment ring cells, and ciliated ring cells. Pigment ring cells and ciliated ring cells combine to form a functional photosensory organ (Fig. 4.25). Figure 4.26 summarises the stages of *Amphimedon queenslandica* embryonic development, tracing the genesis of larval cell types.

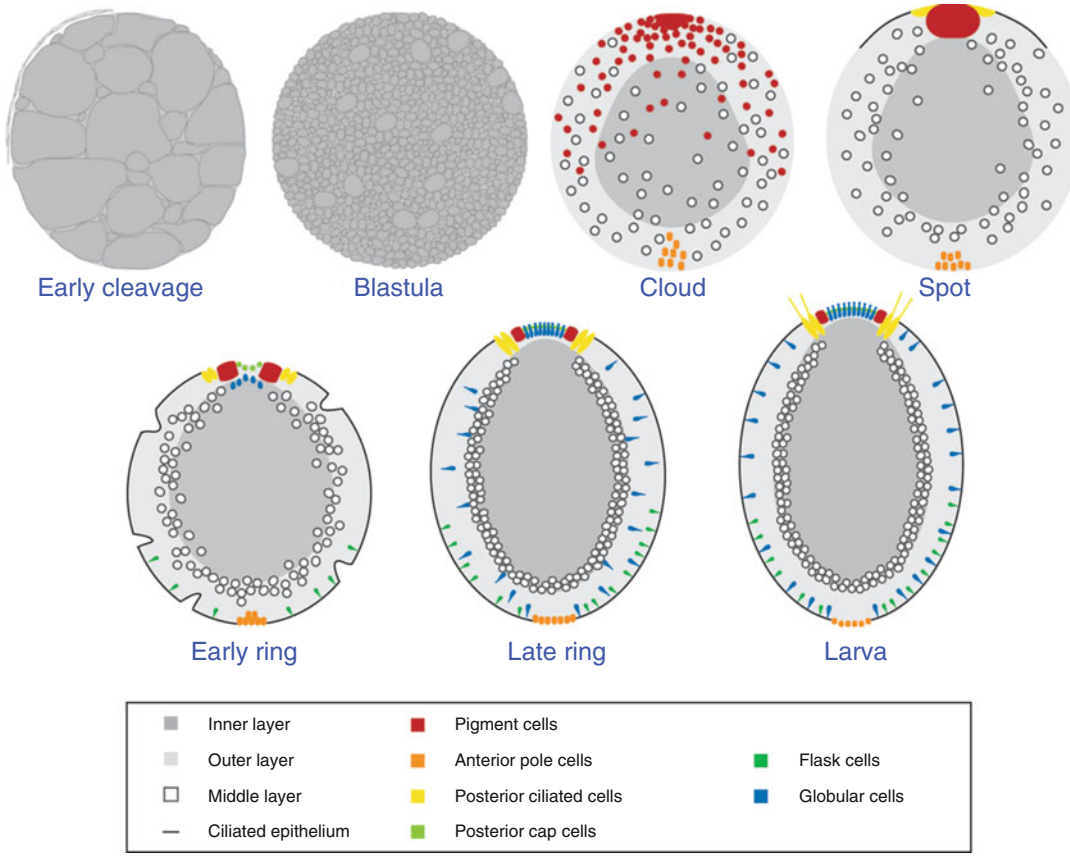

Fig. 4.26 Summary of *Amphimedon queenslandica* development highlighting the ontogeny of selected cell types and regions

Autonomous Formation of Pigment Spots and Rings

The formation of a pigment ring at the posterior end of the larva is essential to the photosensory capabilities of the larva (Leys and Degnan 2001; Rivera et al. 2012). The ring must be in a near-perfect circular pattern for the larva to swim away from light. The developmental mechanisms underlying the formation of this and other sponge tissues remain largely unknown.

Grafting of pigment cells from cloud, spot, and early ring stage embryos to another embryo results in the ectopic formation of pigment spots and rings in the new location (Fig. 4.27). These structures develop in accordance with the location from which they originated, and not the position to which they were transplanted, indicating that the fates of these cells (in larvae) have been determined earlier in development. The ability of these heterotopic grafts to form rings out of the normal spatial context suggests that the formation of pigment rings from spots relies on an intrinsic signalling system and that pigment cells of different ages – from cloud to early ring, at least – have self-organising ability to form an ectopic ring.

Localised and Cell Type-Specific Gene Expression in Late Stage Embryos and Larvae

Many of the genes studied to date in *Amphimedon queenslandica* are differentially expressed in specific cell types or cell layers in spot and ring stage embryos and swimming larvae. The reader is directed to specific publications for detailed descriptions of specific genes (Table 4.3). From late spot/early ring stage to the newly hatched

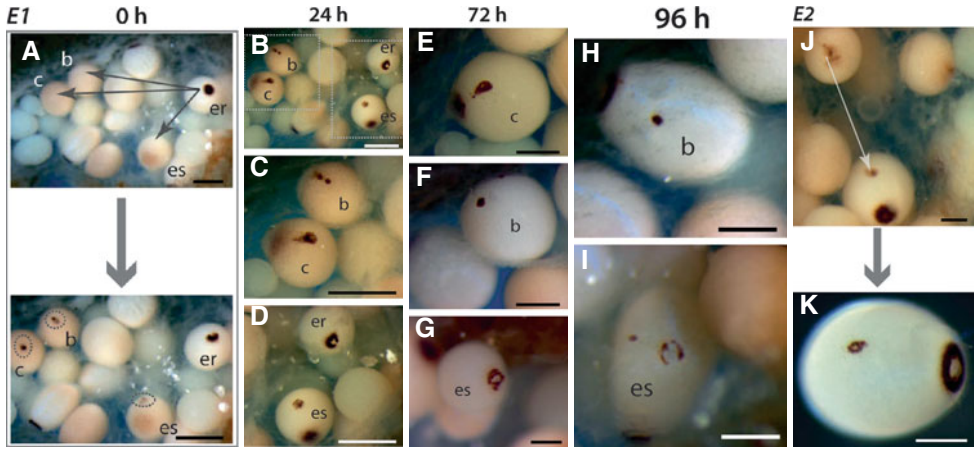

Fig. 4.27 Ectopic formation of pigment spots and rings in heterotopic grafts of pigment cells. Two experiments are shown, *E1* and *E2*. (A–I) In *E1*, pigment and possibly other cells from within the pigment ring of an early ring (*er*) stage embryo are transplanted onto the side of a brown stage embryo (*b*), cloud stage embryo (*c*), and early spot stage embryo (*es*). Manipulated embryos continue to develop in the brood chamber. (**A**) Source and grafted embryos (*arrows*). (**B**–**D**) 24 h post-graft. (**B**) General view of the brood chamber. (**C**, **D**) Higher magnification views of the boxed areas in **B**. Some, but not all, of the transplanted pigment cells in brown and cloud embryos are migrating posteriorly. Pigment cells transplanted into the early spot embryo do not migrate posteriorly. (**E**–**G**) 72 h post-graft. (**E**) Cells that do not migrate posteriorly in brown embryo graft form a small, tight spot. (**F**) Cells that do not migrate posteriorly in cloud embryo graft form a poorly defined spot/ring, which does not change by the end of the experiment. (**G**) Cells transplanted into the early spot embryo form a small ring. (**H**, **I**) 96 h post-graft. (**H**) The pigment spot formed in the brown embryo graft remains small, tight spot. (**I**) The ectopic ring formed on the side of the early spot embryo continues to expand to the point of becoming fragmented. (**J**, **K**) In *E2*, pigment and associated cells from a cloud stage embryo are transplanted onto the side of an early ring stage embryo (**J**) and allowed to develop and hatch as a swimming larva (**K**). Scale bars: (**A**–**D**), 500 μm; (**E**–**K**), 250 μm

Table 4.3 Genes with localised developmental expression patterns in *Amphimedon queenslandica*

Gene and gene family	References
Transcription factors	
Homeobox: *Bsh*; *NK2/3/4*; *NK5/6/7B*; *Tlx*; *Prox2*; *Pax2/5/8*; *POUI*; *Lhx1/5*; *Lhx3/4*	Larroux et al. (2006), Larroux (2007), Fahey et al. (2008), Srivastava et al. (2010b)
GATA: *GATA*	Nakanishi et al. (2014)
Nuclear receptor: *NR1*; *NR2*	Larroux et al. (2006), Bridgham et al. (2010)
Sox: *SoxB*, *C*, *F*	Larroux (2007)
Developmental signalling pathways	
Hedgehog: *Hedgling*	Adamska et al. (2007b)
Notch: *Notch*; *Delta1–5*	Richards et al. (2008), Richards (2010), Richards and Degnan (2012)
TGF-β: *TGF-β*	Adamska et al. (2007a)
Wnt: *WntA-C*; *FzdA*, *B*; *SFRPA*, *C*, *D*; *Lrp5/6*; *GSK*; *APC*; *Axin*; *Dsh*; *β-CatA*; *TCF*; *Gro*	Adamska et al. (2007a, 2010)
Toll pathway	
NF-κB; *TIR1*; *TIR2*; *MyD88*; *Tollip*; *Pellino*	Gauthier and Degnan (2008), Gauthier (2010), Gauthier et al. (2010)
Structural genes	
Cryptochrome: *Cry1*; *Cry2*	Rivera et al. (2012)
Epithelial proteins: *MPP5/7*; *ERM*; *Par-1*, *Par-6*; *Lgl-1*; *p120Catenin*; *Dlg*; *aPKC*	Fahey (2011)
Myosin: *STmyhc*; *NMmyhc*	Steinmetz et al. (2012)
Other: *ferritin*; *procollagen lysyl hydroxylase*; *galectin*	Larroux et al. (2006)
Postsynaptic proteins: *Dlg*; *Grip*; *Homer*; *Gkap*; *Cript*	Sakarya et al. (2007)

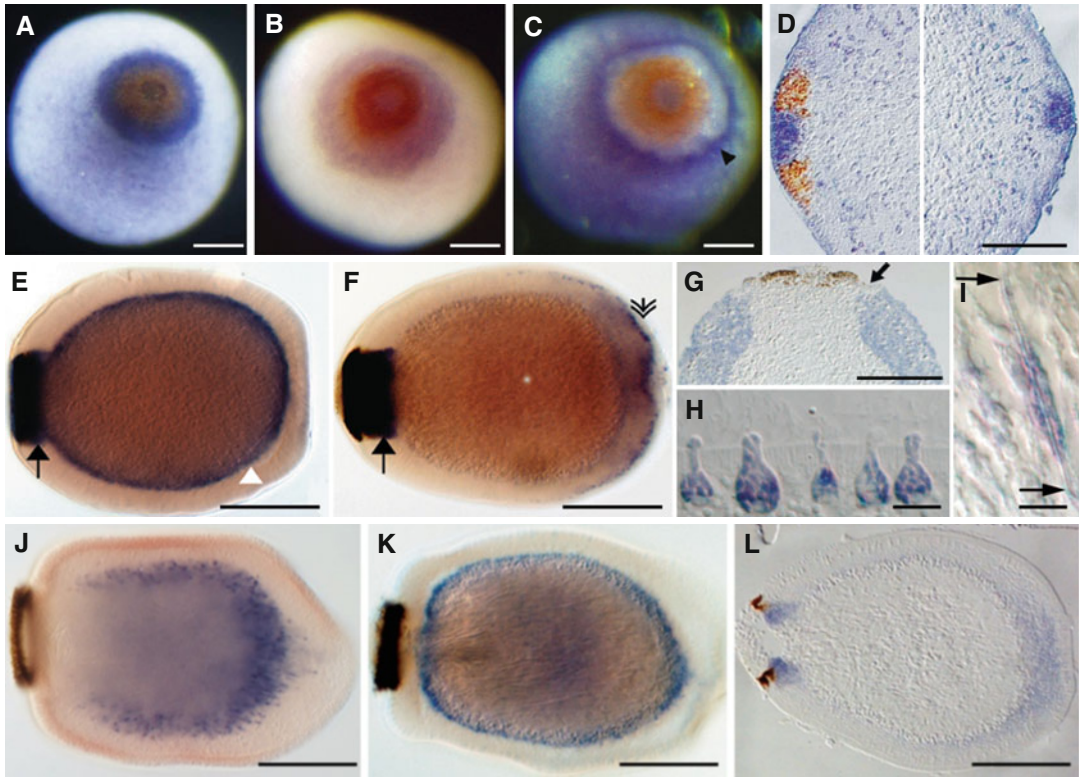

Fig. 4.28 Examples of localised and cell type-specific gene expression in late stage embryos and larvae. (**A**–**D**) Early ring stage. (**E**–**G**) Late ring stage. (**H**–**L**) Swimming larval stage. (**A**) *Cryptochrome 2* (*Cry2*) is expressed around the pigment ring, including long-ciliated cells next to the ring. (**B**) '*Non-muscle*' *type II myosin heavy chain* (*NM myhc*) is more broadly expressed but overlaps with *Cry2* expression. (**C**) '*Striated muscle*' *type II myosin heavy chain* (*ST myhc*) is expressed in the epithelium adjacent to *NM myhc* expression domain. (**D**) *Groucho* (*gro*) expression is enriched in posterior cells inside the ring and cuboidal cells at the most anterior end. (**E**, **F**) *Delta4* is expressed in a dynamic pattern. First (**E**), overlapping with the pigment ring (*black arrow*) and cells at the boundary between inner and outer cell layers (*white arrowhead*). Then (**F**), expression in boundary cells becomes undetectable while appears in the flask cells, which are enriched in the anterior third of the embryo (*double arrow*). (**G**) *p120catenin* is expressed in the forming epithelium but not in the long-ciliated cells expressing *Cry2* (*arrow*). (**H**) *TLR/ILR1-like receptor* (*IgTIR1*), along with many other genes, is expressed in globular cells that migrate late in development from the middle subepithelial layer to the larval surface. (**I**) *Bsh* homeobox is expressed in sclerocytes (*arrows* mark the cell edge). (**J**) *Sox 2* expression is a subset of cells that line the outer region of the inner cell mass. (**K**) *Delta3* in subepithelial cells. (**L**) *Lrp* in cells underlying the pigment ring and anterior epithelial cells. Scale bars: (**A**–**G**, **J**–**L**), 100 μm; (**H**), 10 μm; (**I**), 5 μm (**A**) (From Rivera et al. 2012); (**B**) and (**C**) (From Steinmetz et al. 2012); (**D**, **G** and **L**) (From Adamska et al. 2010); (**E**, **F** and **K**) (From Richards et al. 2012); (**H**) (From Gauthier et al. 2010); (**I**) (From Larroux et al. 2006)

larval stage can be considered a second phase of cell differentiation, which follows from the first phase comprising the formation of pigment cells, sclerocytes, and ciliated epithelial cells during cleavage (see above). These later developmental stages are typified by localised and cell type-restricted expression of transcription factor, signalling pathway, and structural genes (Fig. 4.28). This includes enrichment of innate immunity and neuronal genes in globular cells (Fig. 4.28H Sakarya et al. 2007; Gauthier and Degnan 2008; Richards et al. 2008; Gauthier et al. 2010) and epithelial genes in the larval epithelium (Fig. 4.28G Fahey and Degnan 2010); other outer layer cell types – anterior cuboidal and flask cells – have cell-specific gene expression patterns (Fig. 4.28D, F; e.g., Adamska et al. 2007a, 2010; Richards and Degnan 2012). Restricted expression patterns in the ICM are consistent with there being a number of cryptic cell types in this layer (e.g., *Sox2* is expressed only in a subset of cells on the periphery of the inner cell mass; Fig. 4.28J).

Localised Expression of Conserved Developmental Genes During Pigment Ring Formation

The photosensory capabilities of the posterior pigment ring in the *Amphimedon queenslandica* larva requires the patterning of at least two cell types, the inner pigment cells and the surrounding long-ciliated cells (Figs. 4.6 and 4.26); other cell types that exist in this larval territory include a cell type that may contain both pigment and a long cilium. The expression of *cryptochrome 2* (*Cry2*) in long-ciliated cells is consistent with these being able to detect light (Leys et al. 2002; Rivera et al. 2012). Presumably the pigment cells shade the *Cry2*-expressing cells and thereby attenuate the level of light hitting these cells. This in turn affects the behaviour of the long cilia by an unknown mechanism.

During the migration of the pigment cells to the posterior pole, and especially during spot and ring formation, a raft of signalling ligand and transcription factor genes are differentially expressed in this region (state of knowledge summarised in Fig. 4.29). In addition to *Wnt* and *TGF-β*, which are activated before spot formation (Fig. 4.19), *Hedgling* and two *Delta* ligands are differentially expressed in patterns overlapping with the pigment spot and with adjacent *Cry2*-expressing cells (Fig. 4.29A). Some expression patterns correspond to the boundaries between spot and *Cry2*-expressing (long-ciliated) cells (*Hedgling* and *Delta4*) and *Cry2*-expressing (long-ciliated) and surrounding epithelial cells (*Hedgling* and *TGF-β*), while others do not correspond perfectly to obvious morphological territories (Adamska et al. 2007a, b, 2010; Richards and Degnan 2012). The overlapping expression patterns of signalling ligands in *Amphimedon queenslandica* are reminiscent of many situations in eumetazoan development, suggesting that combinatorial signalling via Wnt, TGF-β, Hedgehog/Hedgling, and Notch pathways is a crown metazoan synapomorphy (reviewed in Adamska et al. 2011).

At this same developmental stage, a diversity of transcription factor genes are activated in the posterior pole (Fig. 4.28B). Many of these genes are expressed in *Cry2*-expressing cells, although some have broader patterns; some overlap directly with a given signalling ligand gene (*Lhx3/4* and *WntA*) or with a combination of signalling ligand genes (*POUI* and *WntA* + *TGF-β* + *Delta4*). Of the conserved transcription factor genes expressed in the vicinity of the *Cry2-expressing* cells, most have eumetazoan orthologs involved in neurogenesis and sensory cell specification (Larroux et al. 2006; Larroux 2007; Richards et al. 2008; Adamska et al. 2010; Richards 2010; Richards and Degnan 2012; Srivastava et al. 2010b). Between spot and ring stages, the posterior expression patterns of many of these genes change, often into broader domains (Fig. 4.28B, C). Although the specific role of these developmental genes is currently unknown in *Amphimedon queenslandica*, their restricted expression in particular cell types is akin to many developmental events in eumetazoans.

SETTLEMENT AND METAMORPHOSIS IN *AMPHIMEDON QUEENSLANDICA*

As is the case with embryogenesis, metamorphosis varies markedly between sponges, although a common set of morphogenetic mechanisms tend to be deployed, e.g., epithelial mesenchyme transition (EMT; see Ereskovsky 2010 for a systematic analysis of sponge metamorphosis).

Competent *Amphimedon queenslandica* larvae undergo rapid metamorphosis when they come in contact with an inductive environmental cue. Typically, larvae require at least 4 h of further development (at 24 °C) after emerging from the mother sponge before they are able to respond to this cue. During this time they are negatively phototactic (Leys and Degnan 2001; Leys et al. 2002), although during the first 2 h they can be observed on occasion swimming upwards towards the surface, which may facilitate dispersal (Degnan and Degnan 2010). A strong inductive cue is associated with the surface of live encrusting and articulated coralline algae (Degnan and Degnan 2010). Upon settling on the algae, larvae undergo a rapid and dramatic reorganisation of the body plan (Fig. 4.30). In *Amphimedon queenslandica*, a functional feeding juvenile is formed in about 3 days after the initiation of metamorphosis. As is the case with most other marine invertebrates, *Amphimedon*

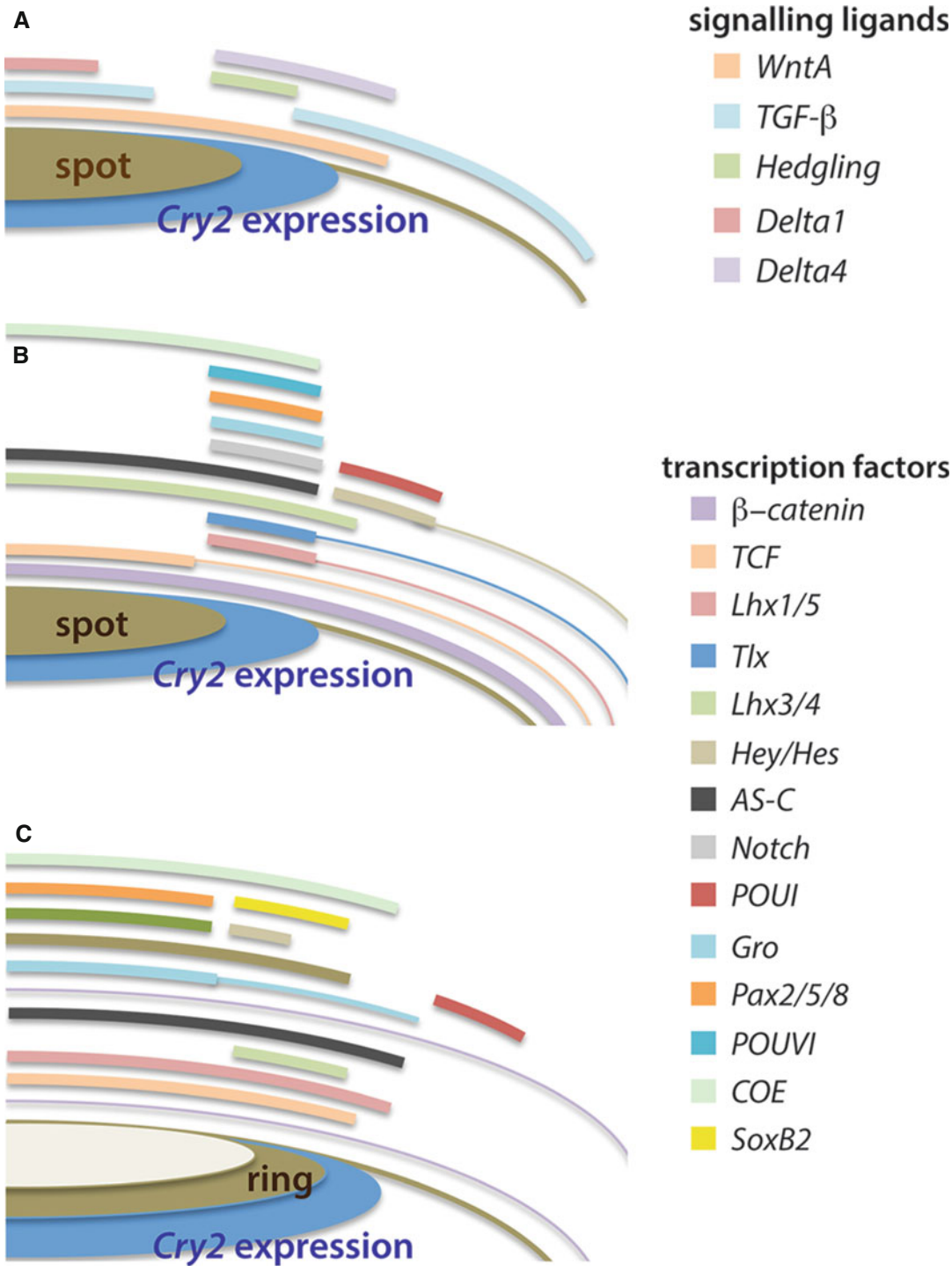

Fig. 4.29 Diagram of localised expression of signalling ligand and transcription factor genes in the vicinity of the pigment spot and ring. One half of the posterior end of spot and ring stage embryos are depicted. (**A**, **B**) Spot stage. (**C**) Ring stage. (**A**) Ligands of Wnt, TGF-β, Notch, and Hedgling pathways are expressed in overlapping patterns with the pigment spot and adjacent *Cry2*-expressing cells. (**B**) Multiple conserved transcription factor genes are expressed in this region, many overlapping with *Cry2*-expressing cells. (**C**) These and other transcription factor genes are co-expressed in this region as the pigment ring forms

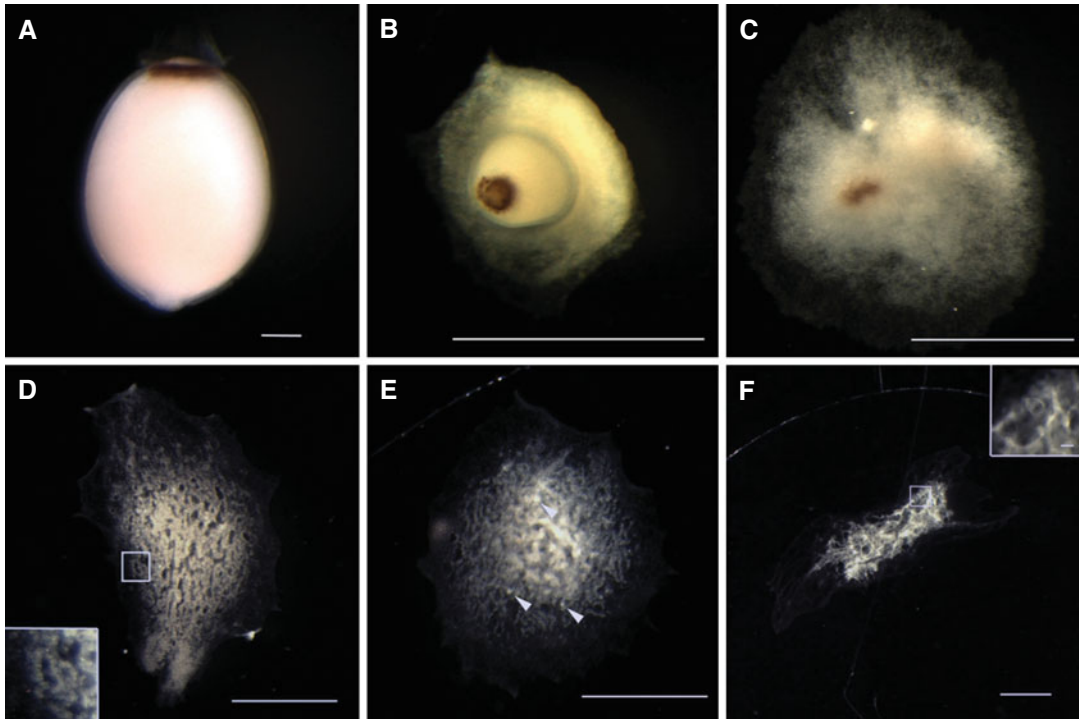

Fig. 4.30 Stages of development during metamorphosis in *Amphimedon queenslandica*. (**A**) Free-swimming parenchymella larva; posterior pigment ring up. (**B–F**) Metamorphosing postlarvae viewed from the top. (**B**) Within 1 h of initiating settlement and metamorphosis. The anterior region of the larva is attached to the substrate, onto which the larva flattens. (**C**) Mat formation, approximately 6 h post-settlement (hps). Cells of the metamorphosing postlarva migrate laterally on the substrate to form a mat-like structure. Note that former posterior pigment ring is diffuse and disappearing. (**D**) Chamber postlarval stage (~48 hps). The aquiferous system composed of canals lined by choanocytes and endopinacocytes first becomes evident. (**E**) Tent-pole-formation postlarval stage (48–72 hps); the exopinacotes covering the outer surface of the metamorphosing postlarva are lifted upwards by formation of tent-pole-like siliceous skeletal elements. Arrowheads show the internal tent-pole-like structures, visible here as clustering of cells. (**F**) Juvenile (rhagon) stage with an osculum (inset), marking the establishment of the functional aquiferous system. Scale bars: (**A**), inset in (**F**), 100 μm; (**B–F**), 1 mm (From Nakanishi et al. 2014)

queenslandica exhibits variation between individual larvae in (i) the timing of the onset of developmental competence to be induced to settle and initiate metamorphosis, (ii) the period of negative photosensitivity, and (iii) the responsiveness to specific environmental cues (e.g., different algae) (Leys and Degnan 2001; Degnan and Degnan 2010).

Within hours of settling, the larva changes into an encrusting mat (Fig. 4.30C). Tracing different populations of labelled larval cells – epithelial, flask, and internal archaeocytes – through metamorphosis reveals that there is no constancy in larval and juvenile cell layers, with all larval cell types apparently capable of transdifferentiating into any juvenile cell type. There is also extensive programmed cell death of epithelial cells at metamorphosis (Fig. 4.31; Nakanishi et al. 2014). In other words, there appears to be no relationship between the cell layers established during embryogenesis and those produced at metamorphosis. In other sponges, the larval epithelial layer has been reported to shed entirely (Bergquist and Green 1977), to be phagocytised by archaeocytes (Meewis 1939; Misevic and Burger 1982, 1990), to differentiate into choanocytes through a non-ciliated amoebocyte intermediate (Amano and Hori 1993, 2001), or to directly differentiate into choanocytes without loss of cilia (Ereskovsky et al. 2007; reviewed in Ereskovsky 2010). Interestingly, the endomesoderm gene *GATA* is consistently expressed in the inner layer of both larvae and juveniles, despite the extensive reorganisation of the body plan at meta-

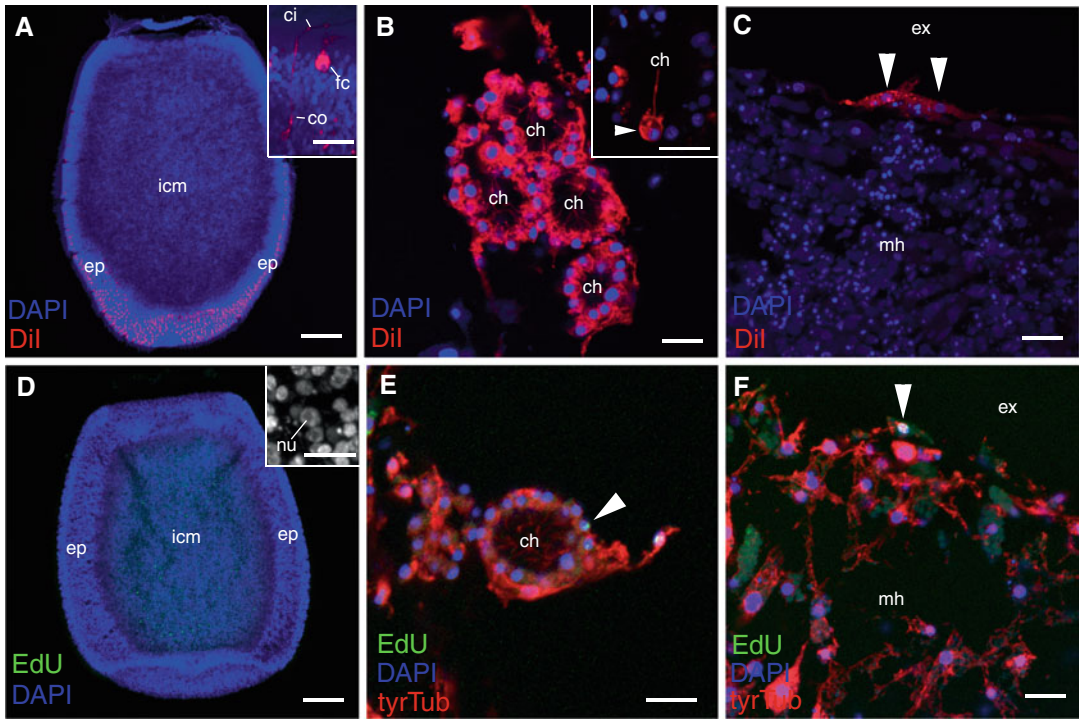

Fig. 4.31 Cell labeling and lineage-tracing through *Amphimedon queenslandica* metamorphosis. (**A**, **D**) Swimming larvae with subsets of cells labelled; anterior is to the *bottom*. (**B**, **C**, **E**, **F**) Descendants of the labelled cells in 3-day-old juveniles. Nuclei are stained with DAPI in all micrographs (*blue*), and in (**E**, **F**), the juveniles are labelled with an antibody against tyrosinated tubulin (tyrTub; *red*). (**A**) Longitudinal confocal sections through the centre of a larva incubated with CM-DiI, showing strong labeling in ciliated epidermal cell types, the columnar epithelial cell (*co*), and the flask cell (*fc*) (*inset*), with little labeling in inner cell mass (*icm*). (**B**) Choanocytes in chambers (*ch*). In some cases, a subset of choanocytes is CM-DiI-labelled in a single choanocyte chamber (*arrowhead* in inset), suggesting that multiple precursor cells can be involved in development of a single chamber. (**C**) Labelled exopinacocytes (*arrowheads*). (**D**) A confocal longitudinal section through the centre of a free-swimming larva pulse-labelled with EdU. Note that the labelled cells localise in the inner cell mass (*icm*) and are likely to be proliferating archaeocytes with characteristic large nucleoli (*nu*). (**E**) An EdU-positive choanocyte in the chamber (*arrowhead*). (**F**) An EdU-positive exopinacocyte (*arrowhead*). Other abbreviations: *ep* outer layer epithelium, *ci* cilium, *ex* external environment, *mh* mesohyl. Scale bars: (**A**, **D**), 100 μm; (**B**, **C**, **E**, **F**), inset in (**D**), 10 μm; inset in (**A**, **B**), 5 μm (From Nakanishi et al. 2014)

morphosis. Labeling of juvenile choanocytes reveals a further lack of cell layer and identity permanency, with these cells dedifferentiating into archaeocytes and transdifferentiating into a range of juvenile cell types, including the outer exopinacoderm (Nakanishi et al. 2014).

THE CALCAREOUS SPONGE *SYCON CILIATUM*

Although *Amphimedon queenslandica* serves as an excellent demosponge model in evolutionary and developmental biology research, the vast evolutionary distance between sponge lineages makes it necessary to include additional model species to represent the remaining lineages. Calcareous sponges have been intensively studied in the past centuries, and analysis of their development has significantly influenced evolutionary theory. For example, Ernst Haeckel coined the term gastrulation and formulated the Gastrea theory, after investigation of development and metamorphosis of a syconoid species from the class Calcaronea (Haeckel 1874; revisited by Leys and Eerkes-Medrano 2005). *Sycon ciliatum*, an abundant North East Atlantic calcaronean sponge, is now emerging as a calcisponge model species, with extensive sequence resources and protocols for gene expression utilised in a variety of studies

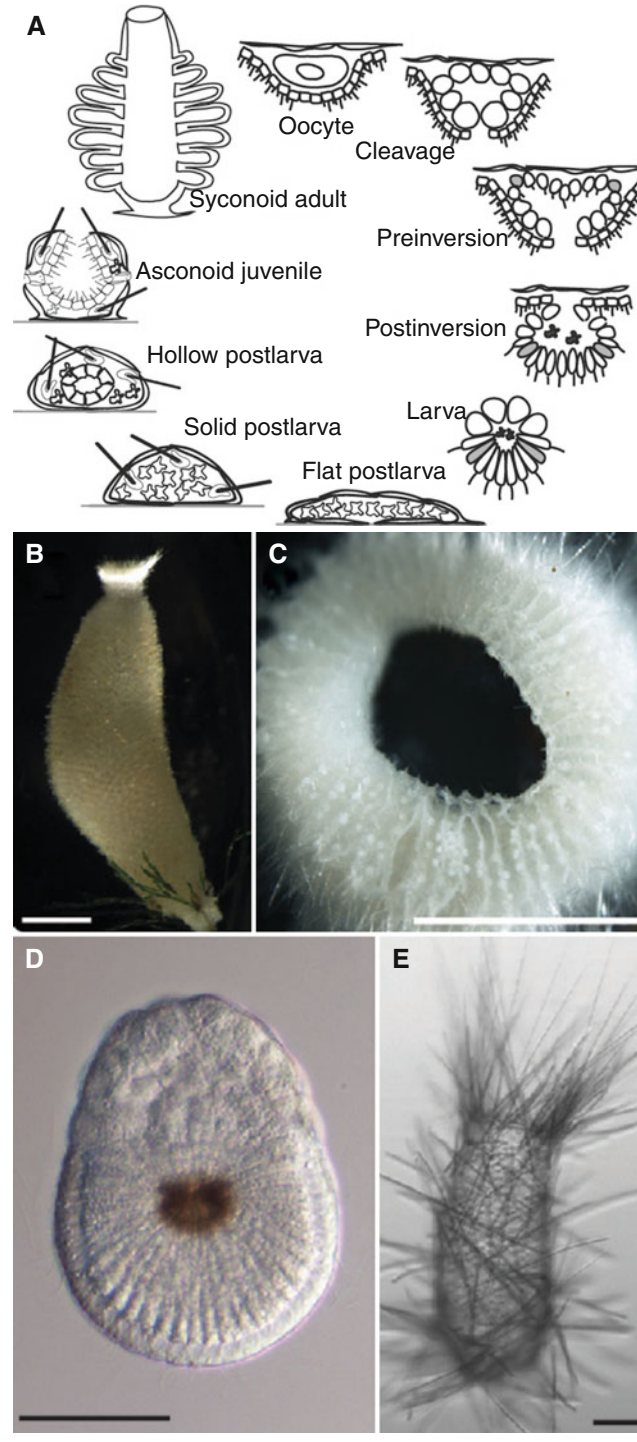

Fig. 4.32 *Sycon ciliatum*, an emerging calcisponge model species. (**A**) Schematic representation of the lifecycle, clockwise from the oocyte to adult. (**B**) Adult specimen. (**C**) Transverse section through a reproductive adult specimen. (**D**) Larva, anterior half composed of micromeres pointing down. (**E**) Juvenile (olynthus). Scale bars: B, C, 5 mm; D, E, 50 µm (Modified from Leininger et al. (2014) and Fortunato et al. (2014))

(Adamska et al. 2011; Fortunato et al. 2012, 2014; Nosenko et al. 2013; Robinson et al. 2013; Sebé-Pedrós et al. 2013; Fortunato 2014; Leininger et al. 2014; Zakrzewski et al. 2014).

The adult specimens of *Sycon ciliatum* are barrel shaped and usually reach 5 cm in length and have a typical syconoid body organisation: choanocyte chambers arranged around the

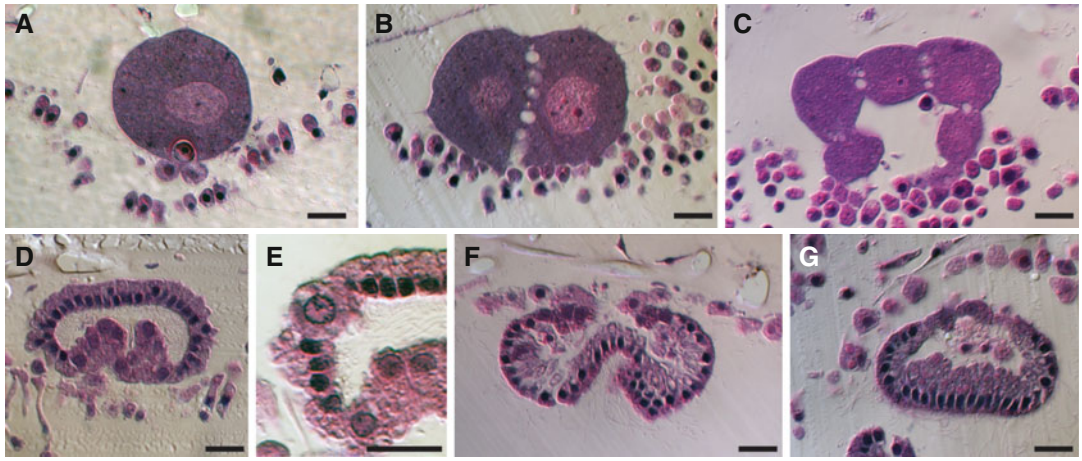

Fig. 4.33 Histological sections through embryonic stages of *Sycon ciliatum*. (**A**) Fertilisation complex. (**B**, **C**) Cleavage. (**D**, **E**) Preinversion. (**E**) Higher magnification demonstrating one of four cruciform cells located between micromeres. (**F**) Embryo soon after inversion, the opening between macromeres still communicated with the gap between accessory cells. (**G**) Postinversion stage, several maternal cells present inside of the embryonic cavity. Scale bars: 10 μm (Modified from Leininger et al. (2014))

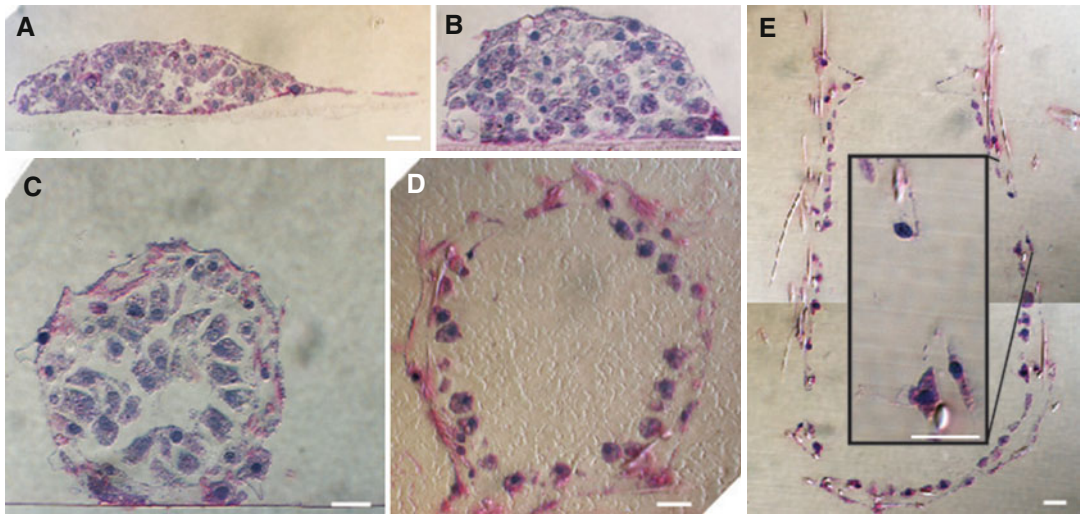

Fig. 4.34 Histological sections through metamorphosis stages of *Sycon ciliatum*. (**A**) Postlarva soon after settlement. (**B**–**D**) Formation of the choanocyte chamber. (**E**) Juvenile, with magnification showing three principal cell types: choanocyte, pinacocyte, and porocyte. Scale bars: 10 μm

central atrium (Fig. 4.32A–C). As for all calcisponges, it is viviparous with embryogenesis occurring in the narrow mesohyl layer between the outer pinacoderm and the inner choanoderm (Figs. 4.32C and 4.33). The larva ('amphiblastula') is approximately 100 μm long and is transparent, except for pigment deposited within the basal (inner) tips of the micromeres (Fig. 4.32D). It is composed of two major cell types: the numerous micromeres comprising the anterior part of the larva have flagella, in contrast to the larger and less numerous macromeres at the posterior pole (Fig. 4.32A, D). In contrast to the rhagon, the putative phylotypic juvenile stage of demosponges, the calcisponge juvenile has only a single choanocyte chamber (Figs. 4.32A, E and 4.34) and is referred to as the olynthus (Ereskovsky 2010). *S. ciliatum* is one of the few sponge species that maintains radial symmetry throughout its life.

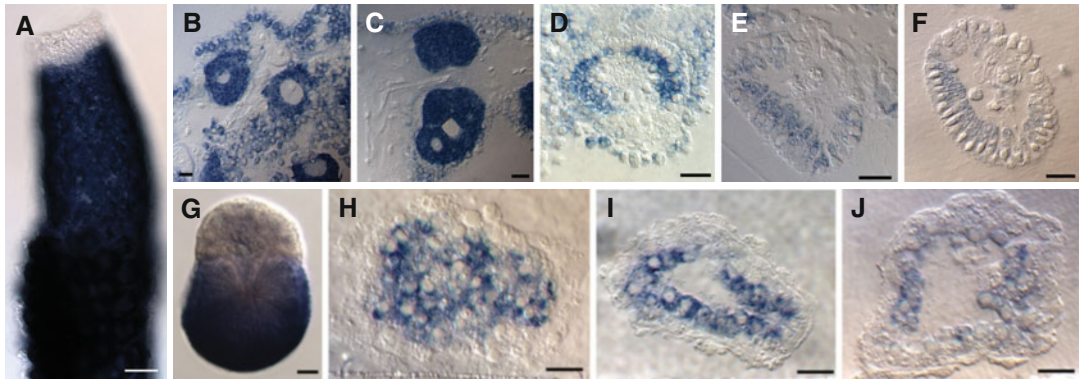

Fig. 4.35 Expression of *Tubulin*-β in *Sycon ciliatum* marks ciliated cells and early embryos. (**A**) Young adult with strongly labelled choanocytes. (**B**–**F**) Sections showing oocytes, cleavage, preinversion, and early and late postinversion stage embryos. (**G**) Larva with strong expression in micromeres and negative macromeres. (**H**–**J**) Sections showing expression in the inner cell mass and differentiating choanocytes during metamorphosis. Scale bars: (**A**), 100 μm; (**B**–**J**), 10 μm

Recent and ongoing studies demonstrate significant differences in the content of developmental regulatory genes (i.e., the developmental toolkit) between *Amphimedon queenslandica* and *Sycon ciliatum* (Fortunato et al. 2012, 2014; Sebé-Pedrós et al. 2013; Fortunato 2014; Leininger et al. 2014). In a majority of cases, the genome of *S. ciliatum* contains more protein family members than *A. queenslandica*: 21 versus 3 Wnt ligands, 22 versus 8 TGF-β ligands (Leininger et al. 2014), and 7 versus 4 Sox transcription factors (Fortunato et al. 2012). In addition, *S. ciliatum* possesses several developmental genes that are absent from *A. queenslandica*, for example, *Eyes absent* (Fortunato et al. 2014). In other gene families, the two species share different paralogs with bilaterians: for example, T-box family genes *Brachyury* and *Eomes* are present in *S. ciliatum*, while *Tbox4/5* and *TboxPor* are present in *A. queenslandica* (Sebé-Pedrós et al. 2013). This complex picture appears more consistent with multiple independent gene family expansions and gene losses in sponge lineages than with being simply explained by sponge paraphyly (Fortunato 2014).

SYCON CILIATUM DEVELOPMENT

Development of calcaronean sponges has several unique features, beginning with fertilisation that is assisted by specialised cells of the mother sponge, called carrier cells (reviewed in Ereskovsky 2010). The oocytes are positioned between the pinacocyte and choanocyte layers; choanocytes directly overlying the oocytes lose their collars and become accessory cells. As a sperm cell penetrates into one of the accessory cells, this cell becomes a carrier cell. The sperm cell inside of the carrier cell is referred to as a spermiocyst and is transferred into the oocyte to complete fertilisation (Fig. 4.33A). Intriguingly, while 100 % of *Sycon ciliatum* specimens collected in May in the Norwegian fjords contain oocytes and a majority of those collected over a few days in late May contained fertilisation complexes, spermatogenesis was not observed despite frequent sampling over several years (Leininger et al. 2014 and unpublished observations). The development that follows fertilisation is also semi-synchronous across the *S. ciliatum* population, with individual sponges 'lagging behind' no more than a few days. This leads to the release of larvae at the end of June and beginning of July (Leininger et al. 2014).

Embryogenesis of calcaronean sponges is well described on light and electron microscopy levels (Amano and Hori 1992, 1993; Franzen 1988; Eerkes-Medrano and Leys 2006; reviewed in Ereskovsky 2010). Early cleavage is highly stereotypic, and up to the eight-cell stage, the embryo has a rhomboid shape with all blastomeres positioned in the plane defined by the choanocyte and pinacocyte layers (Figs. 4.32A, 4.33B, 4.35C, and 4.36A, B, G, I, N). Cytoplasmic bridges are initially maintained between

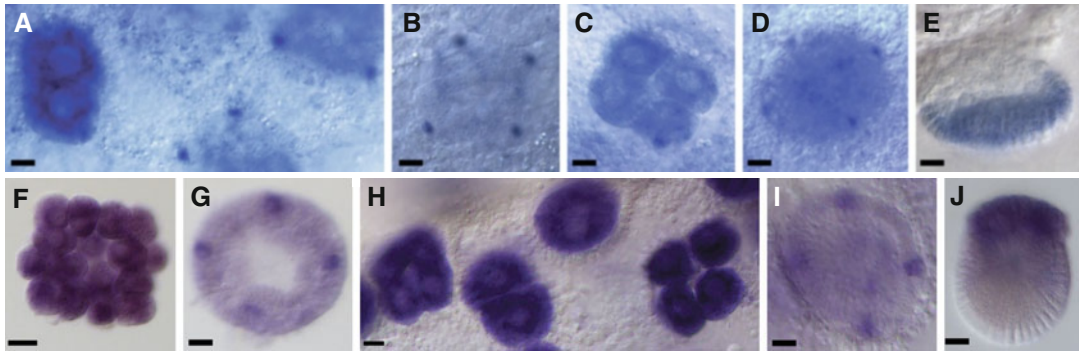

Fig. 4.36 Expression of cruciform cell markers in *Sycon ciliatum*. (**A**, **B**) *DvlB* transcripts become localised to cross cells during cleavage. (**C**–**E**) *DvlA* transcripts are stronger in the cross cells than in the remaining blastomeres and are then detectable in micromeres of postinversion stage embryos. (**F**, **G**) *SoxL1* transcripts and (**H**, **I**) *SoxB* transcripts are uniformly distributed during cleavage and become specific to the cross cells in preinversion stage embryos. (**J**) In the larvae, *SoxB* is detectable in the macromeres only. Scale bars: 10 μm (Modified from Leininger et al. (2014) and Fortunato et al. (2012))

blastomeres (Figs. 4.33B, C, 4.35C, and 4.36A, B). Subsequent divisions result in formation of a cup-shaped 'stomoblastula' embryo, its opening communicating with an opening formed between the accessory cells. When cell differentiation is completed, the embryo is composed of three cell types: large, granular, non-ciliated macromeres adjacent to the choanocytes; smaller and more numerous micromeres, which have cilia pointing into the embryonic cavity; and four cruciform cells, which convey a unique tetraradial symmetry to the embryos (Figs. 4.32A, 4.33D, E, and 4.36). The embryo then undergoes inversion, which will both translocate it into the radial chamber and position the cilia on the outer surface of the larva. During this stage, a small number of maternally derived cells crawl into the larval cavity (Figs. 4.32A, 4.33G, 4.35E, F, and 4.37A, I, D, E, M, O, P; Franzen 1988; Ereskovsky 2010; Leininger et al. 2014).

Larvae released in laboratory conditions swim close to the water surface during the first 12–24 h post spawning and subsequently begin to search for an appropriate substrate for settlement. During metamorphosis, the larva settles on the anterior pole; within minutes the ciliated cells of the anterior half undergo epithelial-to-mesenchymal transition and form the inner cell mass (Figs. 4.32A and 4.34A). In contrast, the macromeres maintain their epithelial organisation, completely enclose the micromeres, and become the pinacocytes of the forming juvenile. The cross cells and the maternal cells degenerate soon after settlement (Amano and Hori 1993). Sclerocytes differentiate quickly within the inner cell mass and spicule production starts approximately 12 h after settlement. A single choanocyte chamber forms, and the postlarva expands by increasing the volume of the chamber and thinning its walls, so they are finally composed of two epithelial layers – the outer pinacoderm and the inner choanoderm, with narrow mesohyl sparsely populated with sclerocytes and other not well-characterised cell types in between (Figs. 4.32A, 4.34B–D, and 4.35H–J). Finally, the osculum opens, and the juvenile sponge acquires ascon-level organisation with porocytes providing connections (ostia) between choanoderm and pinacoderm (Figs. 4.32A, E and 4.34E). As the asconoid body plan gives rise to the syconoid body plan during subsequent growth, choanocytes of the original choanocyte chamber become replaced with endopinacocytes in the region where radial chambers form. In terms of morphology and directionality of the water flow, the radial chambers are reminiscent of the original juvenile and can be treated as serially homologous to the olynthus (Manuel 2001; Leininger et al. 2014).

Extensive gene expression analyses, based on a combination of quantitative transcriptome analysis and in situ hybridisation studies, have provided important clues regarding the homology of cell types and body plans between sponges and

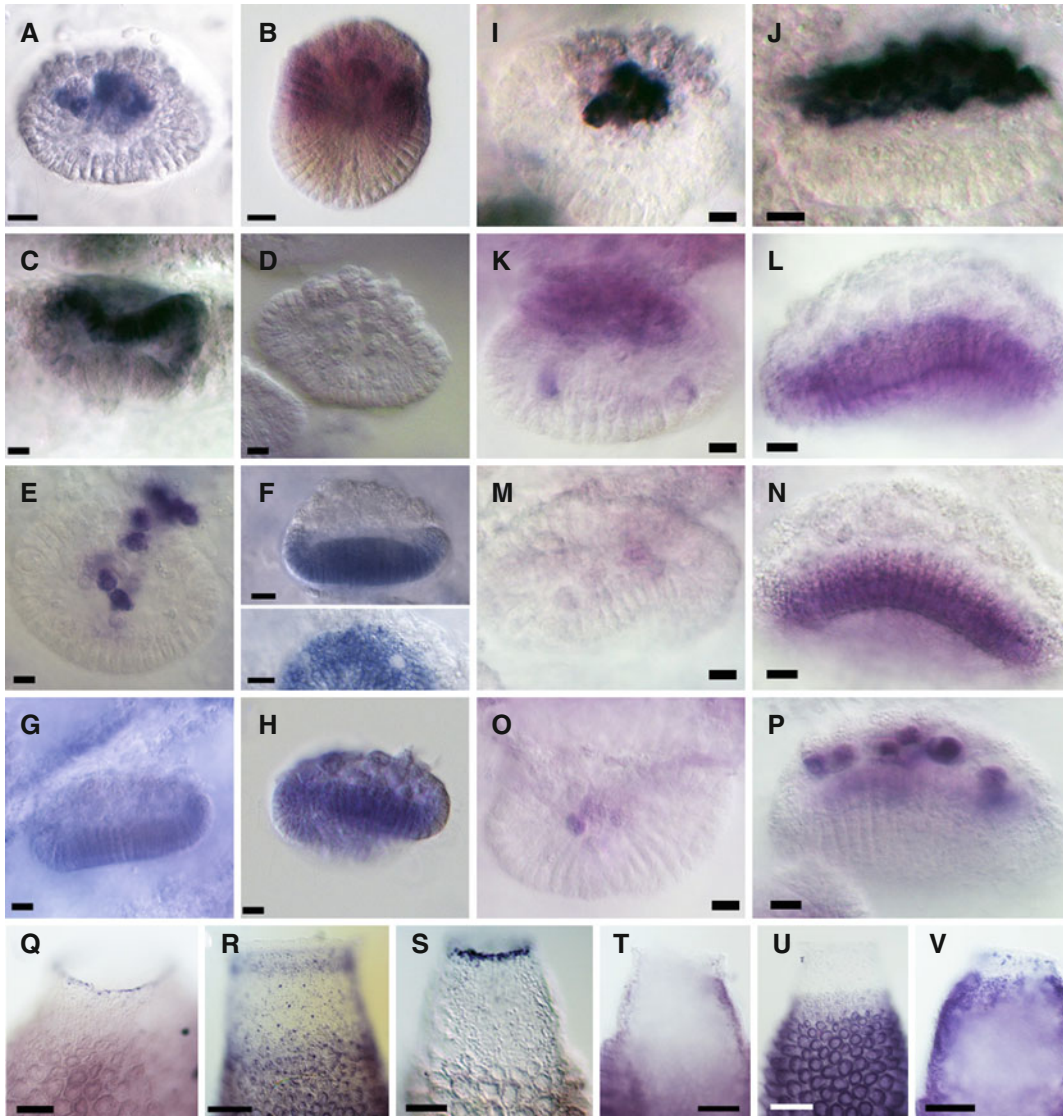

Fig. 4.37 Expression of Wnt and TGF-β pathways components in *Sycon ciliatum*.(**A**) Expression of *WntF* in the maternal cells within postinversion stage embryo. (**B**) Expression of *WntA* in macromeres and posterior micromeres of the larva. (**C**, **D**) Transient expression of β-*cateninA* in micromeres of preinversion stage embryos. (**E**) Expression of β-*cateninB* in maternal cells migrating into embryonic cavity. (**F**, **G**) Expression of *FzdA* and *FzdD* in micromeres. (**H**) Uniform embryonic expression of *TcfB*. (**I**) Strong expression of *TGF-βF* in maternal cells and its weaker expression in the macromeres. (**J**) Strong macromere expression of *TGF-βD*. (**K**, **L**) Expression of *Smad1/5* in macromeres plus cross cells and micromeres of early and late postinversion stage embryos, respectively. (**M**, **N**) Maternal cells and micromere expression of *Smad4* in early and late postinversion stage embryos, respectively. (**O**, **P**) Maternal cell expression of *R-Smad*. (**G**–**V**) *WntG*, *FzdD*, *TGF-βU*, *Smad4*, *Smad15*, and *SmadR* expression in the upper parts of young adult sponges. Scale bars: (**A**–**P**), 10 μm; (**Q**–**V**), 100 μm (Modified from Leininger et al. (2014))

eumetazoans. Several genes involved in specification of neuronal and sensory cells in cnidarians and bilaterians are expressed during differentiation of the cruciform cells, which are suggested to be the sensory cells of the calcaronean larvae (Tuzet 1973). These genes include

SoxB, *PaxB*, *SixC*, *Elav*, *Msi* and *Nanos*, *Hmx*, and other NK-related homeobox transcription factors, as well as several components of the Wnt signalling pathway (Fig. 4.36; Fortunato et al. 2012, 2014; Fortunato 2014; Leininger et al. 2014). Genes involved in specification of the cnidarian and bilaterian endomesoderm are expressed in the embryonic micromeres (which give rise to the choanoderm) and choanoderm of the adult sponges. These include downstream components of the Wnt and TGF-β signalling pathways as well as *Brachyury* and *GATA* transcription factors (Fig. 4.37; Leininger et al. 2014). Finally, numerous Wnt and TGF-β ligands are expressed in the posterior region of the larvae and around the osculum of the adults, highly reminiscent of expression patterns observed in cnidarians and supporting homology of the larval and adult body axes as postulated by Haeckel (1870) (Fig. 4.37; Leininger et al. 2014).

OPEN QUESTIONS

- Is Porifera monophyletic and the sister phylum to all other extant metazoans? Particularly intriguing is the inability to convincingly determine whether sponges or ctenophores are the earliest branching phyletic lineage. One of the standout features when comparing the *Amphimedon queenslandica* genome with ctenophore genomes is the remarkable similarity in developmental and other (e.g., neuronal) gene repertoires. Indeed, the gene content similarity between ctenophores and *Amphimedon queenslandica* might be greater than that between *A. queenslandica* and *Sycon ciliatum*.
- How does sponge embryogenesis and metamorphosis relate to hallmarks of eumetazoan and bilaterian development, including gastrulation and germ layers?
- Are the cell layers observed in sponges homologous to bilaterian germ layers, and if so, is the generative mechanism for the establishment of these layers conserved across the animal kingdom? Even amongst the co-authors of this chapter, there is no agreement. Regardless, it is clear there exists an ancient developmental gene toolkit that is still in use in all animals. This includes conserved signalling pathways whose differential expression contributes to define body plan axes and embryonic territories (e.g., Wnt, Notch) and transcription factors whose expression correlates with the establishment of a cell layer or type (e.g., GATA). The level at which these developmental similarities are homologous to eumetazoan processes remains an open question.

Acknowledgements Because of space limitations, we are unable to cite many important contributions to the field of sponge developmental biology – we acknowledge these here. We also acknowledge the fine contributions of past and present members of the laboratories of B. Degnan, S. Degnan, and M. Adamska towards our understanding of *Amphimedon* and *Sycon* biology. Research presented in this chapter was made possible by the generous support of the Australian Research Council to BMD, SMD, and MA and the Sars International Centre for Marine Molecular Biology to MA.

References

Adamska M, Degnan SM, Green KM, Adamski M, Craigie A, Larroux C, Degnan BM (2007a) Wnt and TGF-β expression in the sponge *Amphimedon queenslandica* and the origin of metazoan embryonic patterning. PLoS ONE 2:e1031

Adamska M, Matus DQ, Adamski M, Green K, Rokhsar DS, Martindale MQ, Degnan BM (2007b) The evolutionary origin of hedgehog proteins. Curr Biol 17:R836–R837

Adamska M, Larroux C, Adamski M, Green K, Lovas E, Koop D, Richards GS, Zwafink C, Degnan BM (2010) Structure and expression of conserved Wnt pathway components in the demosponge *Amphimedon queenslandica*. Evol Dev 12:492–518

Adamska M, Zwafink C, Green K, Degnan BM (2011) What sponges can tell us about the evolution of developmental processes. Zoology 114:1–10

Amano S, Hori I (1992) Metamorphosis of calcareous sponges. 1. Ultrastructure of free-swimming larvae. Invert Reprod Dev 21:81–90

Amano S, Hori I (1993) Metamorphosis of calcareous sponges. 2. Cell rearrangement and differentiation in metamorphosis. Invert Reprod Dev 24:13–26

Amano S, Hori I (2001) Metamorphosis of coeloblastula performed by multipotential larval flagellated cells in the calcareous sponge *Leucosolenia laxa*. Biol Bull 200:20–32

Anavy L, Levin M, Khair S, Nakanishi N, Fernandez-Valverde SL, Degnan BM, Yanai I (2014) BLIND ordering of large-scale transcriptomic developmental timecourses. Development 141:1161–1166

Bergquist PR, Green CR (1977) Ultrastructural-study of settlement and metamorphosis in sponge larvae. Cahiers Biol Mar 18:289–302

Boury-Esnault N, Efremova S, Bézac C, Vacelet J (1999) Reproduction of a hexactinellid sponge: first description of gastrulation by cellular delamination in the Porifera. Invert Reprod Dev 35:187–201

Bridgham JT, Eick GN, Larroux C, Deshpande K, Harms MJ, Gauthier ME, Ortlund EA, Degnan BM, Thornton JW (2010) Protein evolution by molecular tinkering: diversification of the nuclear receptor superfamily from a ligand-dependent ancestor. PLoS Biol 8:e1000497

Degnan SM, Degnan BM (2006) The origin of the pelagobenthic metazoan life cycle: what's sex got to do with it? Integr Comp Biol 46:683–690

Degnan SM, Degnan BM (2010) The initiation of metamorphosis as an ancient polyphenic trait and its role in metazoan life cycle evolution. Phil Trans R Soc B 365:641–651

Degnan BM, Leys SP, Larroux C (2005) Sponge development and antiquity of animal pattern formation. Integr Comp Biol 45:335–341

De Vos L, Rutzler K, Boury-Esnault N, Donadey C, Vacelet J (1991) Atlas of sponge morphology. Smithsonian Institution Press, Washington D.C. 128 pp

Eerkes-Medrano DI, Leys SP (2006) Ultrastructure and embryonic development of a syconoid calcareous sponge. Invert Biol 125:177–194

Ereskovsky AV, Boury-Esnault N (2002) Cleavage pattern in Oscarella species (Porifera, Demospongiae, Homoscleromorpha): transmission of maternal cells and symbiotic bacteria. J Nat Hist 36:1761–1775

Ereskovsky A (2010) The comparative embryology of sponges. Springer, Netherlands

Ereskovsky AV, Tokina DB, Bezac C, Boury-Esnault N (2007) Metamorphosis of cinctoblastula larvae (Homoscleromorpha, Porifera). J Morphol 268: 518–528

Erwin DH, Laflamme M, Tweedt SM, Sperling EA, Pisani D, Peterson KJ (2011) The Cambrian conundrum: early divergence and later ecological success in the early history of animals. Science 334:1091–1097

Fahey B (2011) Origin of animal epithelia: insights from the genome of the demosponge *Amphimedon queenslandica.* PhD Thesis The University of Queensland

Fahey B, Degnan BM (2010) Origin of animal epithelia: insights from the sponge genome. Evol Dev 12:601–617

Fahey B, Larroux C, Woodcroft BJ, Degnan BM (2008) Does the high gene density in the sponge NK homeobox gene cluster reflect limited regulatory capacity? Biol Bull 214:205–217

Fell PE (1969) The involvement of nurse cells in oogenesis and embryonic development in the marine sponge, Haliclona ecbasis. J Morph 127:133–150.

Fortunato SAV (2014) Gene loss, lineage specific expansions and dynamic expression of developmental transcription factors in calcareous sponges. PhD Thesis University of Bergen

Fortunato S, Adamski M, Bergum B, Guder C, Jordal S, Leininger S, Zwafink C, Rapp HT, Adamska M (2012) Genome-wide analysis of the sox family in the calcareous sponge *Sycon ciliatum*: multiple genes with unique expression patterns. EvoDevo 23:142012

Fortunato S, Leininger S, Adamska M (2014) Evolution of the Pax-Six-Eya-Dach network: the calcisponge case study. EvoDevo 5:23

Fortunato S, Adamski M, Mendivil O, Leininger S, Liu J, Ferrier DEK, Adamska M. Calcisponges have a ParaHox gene and dynamic expression of dispersed NK homeobox genes. Nature 514:620–623

Franzen W (1988) Oogenesis and larval development of *Scypha ciliata* (Porifera, Calcarea). Zoomorphology 107:349–357

Funayama N (2012) The stem cell system in demosponges: suggested involvement of two types of cells: archeocytes (active stem cells) and choanocytes (food-entrapping flagellated cells). Dev Genes Evol 223:23–38

Gauthier MEA (2010) Developing a sense of self: exploring the evolution of immune and allorecognition mechanisms in metazoans using the demosponge *Amphimedon queenslandica.* PhD Thesis The University of Queensland

Gauthier M, Degnan BM (2008) The transcription factor NF-κB in the sponge *Amphimedon queenslandica*: insights into the evolutionary origin of the Rel homology domain. Dev Genes Evol 218:23–32

Gauthier MEA, Du Pasquier L, Degnan BM (2010) The genome of the sponge *Amphimedon queenslandica* provides new perspectives into the origin of Toll-like and Interleukin1 receptor pathways. Evol Dev 12:519–533

Gazave E, Lapebie P, Ereskovsky AV, Vacelet J, Renard E, Cardenas P, Borchiellini C (2012) No longer demospongiae: homoscleromorpha formal nomination as a fourth class of Porifera. Hydrobiologia 687:3–10

Gonobobleva EL, Ereskovsky AV (2004) Metamorphosis of the larva of Halisarca dujardini (Demospongiae, Halisarcida). Bull Inst R Sci Nat.Belg 74:101–114

Haeckel E (1870). Ueber den Organismus der Schwame und ihre Verwndtschaft mit den Corallen. Jena Zeitsch Naturwiss 5:207–235

Haeckel E (1874) Die Gastrae Theorie, die phylogenetische Classification des Thierreichs und die Homologie der Keimblatter. Jena Zeitsch Naturwiss 8:1–55

Hayward DC, Samuel G, Pontynen PC, Catmull J, Saint R, Miller DJ, Ball EE (2002) Localized expression of a dpp/BMP2/4 ortholog in a coral embryo. Proc Natl Acad Sci USA 99:8106–8111

Hentschel U, Piel J, Degnan SM, Taylor MW (2012) Genomic insights into the marine sponge microbiome. Nature Rev Microbiol 10:641–654

Hill MS, Hill AL, Lopez J, Peterson KJ, Pomponi S, Diaz MC, Thacker RW, Adamska M, Boury-Esnault N, Cárdenas P, Chaves-Fonnegra A, Danka E, De Laine BO, Formica D, Hajdu E, Lobo-Hajdu G, Klontz S, Morrow CC, Patel J, Picton B, Pisani D, Pohlmann D, Redmond NE, Reed J, Richey S, Riesgo A, Rubin E, Russell Z, Rützler K, Sperling EA, di Stefano M, Tarver JE, Collins AG (2013) Reconstruction of family-level phylogenetic relationships within Demospongiae (Porifera) using nuclear encoded housekeeping genes. PLoS ONE 8:e50437

Hooper JNA, Van Soest RWM (eds) (2002) Systema Porifera, vol 1, A guide to the classification of sponges. Kluwer Academic/Plenum Publishers, New York, xlvii, 1708

Kaye HR (1990) Reproduction in West Indian commercial sponges: oogenesis, larval development, and behavior. In: new Perspectives in sponge biology. Rützler K, ed., Smithsonian Institution Press, Washington DC:161–169

Kaye HR, Reiswig HM (1991) Sexual reproduction in four Caribbean commercial sponges. II. Oogenesis and transfer of bacterial symbionts. lnvert Reprod Dev 19:1–11

Knoblich JA (2010) Asymmetric cell division: recent developments and their implications for tumour biology. Nat Rev Mol Cell Biol 11:849–860

Larroux C (2007) Genome content and developmental expression of transcription factor genes in the demosponge *Amphimedon queenslandica*: insights into the Ancestral Metazoan Developmental Program. PhD Thesis The University of Queensland

Larroux C, Fahey B, Liubicich D, Hinman VF, Gauthier M, Gongora M, Green K, Wörheide G, Leys SP, Degnan BM (2006) Developmental expression of transcription factor genes in a demosponge: insights into the origin of metazoan multicellularity. Evol Dev 8:150–173

Larroux C, Fahey B, Degnan SM, Adamski M, Rokhsar DS, Degnan BM (2007) The NK homeobox gene cluster predates the origin of Hox genes. Curr Biol 17:706–710

Leininger S, Adamski M, Bergum B, Guder C, Liu J, Laplante M, Bråte J, Hoffmann F, Fortunato S, Jordal S, Rapp HT, Adamska M (2014) Developmental gene expression provides clues to relationships between sponge and eumetazoan body plans. Nat Commun 5:3905

Leys SP (2004) Gastrulation in sponges. In Gastrulation, From Cells to Embryo. Edited by Stern CD. New York: cold Spring Harbor Laboratory Press:23–31

Leys SP, Degnan BM (2001) The cytological basis of photoresponsive behavior in a sponge larva. Biol Bull 201:323–338

Leys SP, Degnan BM (2002) Embryogenesis and metamorphosis in a haplosclerid demosponge: gastrulation and transdifferentiation of larval ciliated cells to choanocytes. Invert Biol 121:171–189

Leys SP, Eerkes-Medrano D (2005) Gastrulation in calcareous sponges: in search of Haeckel's gastraea. Integ Comp Biol 45:342–351

Leys SP, Ereskovsky AV (2006) Embryogenesis and larval differentiation in sponges. Can. J. Zool. 84:262–287

Leys SP, Hill A (2012) The physiology and molecular biology of sponge tissues. Adv Mar Biol 62:1–56

Leys SP, Cronin TW, Degnan BM, Marshall JN (2002) Spectral sensitivity in a sponge larva. J Comp Physiol A 188:199–202

Maldonado M, Bergquist PR (2002) Phylum Porifera. In: atlas of marine invertebrate larvae. Young CM, ed, Academic press, London:21–50

Manuel M (2001) Origine et évolution des mécanismes moléculaires contrôlant la morphogenèse chez les Métazoaires: un nouveau modèle spongiaire, *Sycon raphanus* (Calcispongia, Calcaronea). PhD Thesis Université de Paris XI

Maritz K, Calcino A, Fahey B, Degnan BM, Degnan SM (2010) Remarkable consistency of larval supply in the spermcast-mating demosponge *Amphimedon queenslandica* (Hooper and van Soest). Open Mar Biol J 4:57–64

Matus DQ, Pang K, Marlow H, Dunn CW, Thomsen GH, Martindale MQ (2006) Molecular evidence for deep evolutionary roots of bilaterality in animal development. Proc Natl Acad Sci USA 103:11195–11200

McFall-Ngai M, Hadfield MG, Bosch TC, Carey HV, Domazet-Lošo T, Douglas AE, Dubilier N, Eberl G, Fukami T, Gilbert SF, Hentschel U, King N, Kjelleberg S, Knoll AH, Kremer N, Mazmanian SK, Metcalf JL, Nealson K, Pierce NE, Rawls JF, Reid A, Ruby EG, Rumpho M, Sanders JG, Tautz D, Wernegreen JJ (2013) Animals in a bacterial world, a new imperative for the life sciences. Proc Natl Acad Sci U S A 110:3229–3236

Medioni C, Mowry K, Besse F (2012) Principles and roles of mRNA localization in animal development. Development 139:3263–3276

Meewis H (1939) Contribution a l'étude de l'embryogenése de Chalinulidae: haliclona limbata. Ann Soc R Zool Belg 70:201–243

Misevic GN SV, Burger MM (1990) Larval metamorphosis of Microciona prolifera: evidence against the reversal of layers. In: Rt K (ed) New perspectives in sponge biology. Smithsonian Institution Press, Washington, DC, pp 182–187

Misevic GN, Burger MM (1982) The molecular basis of species specific cell-cell recognition in marine sponges, and a study on organogenesis during metamorphosis. Prog Clin Biol Res B 85:193–209

Moroz LL, Kocot KM, Citarella MR, Dosung S, Norekian TP, Povolotskaya IS, Grigorenko AP, Dailey C, Berezikov E, Buckley KM, Ptitsyn A, Reshetov D, Mukherjee K, Moroz TP, Bobkova Y, Yu F, Kapitonov VV, Jurka J, Bobkov YV, Swore JJ, Girardo DO, Fodor A, Gusev F, Sanford R, Bruders R, Kittler E, Mills CE, Rast JP, Derelle R, Solovyev VV, Kondrashov FA, Swalla BJ, Sweedler JV, Rogaev EI,

Halanych KM, Kohn AB (2014) The ctenophore genome and the evolutionary origins of neural systems. Nature 510:109–114

Nakanishi N, Sogabe S, Degnan BM (2014) Evolutionary origin of gastrulation: insights from sponge development. BMC Biol 12:26

Nosenko T, Schreiber F, Adamska M, Adamski M, Eitel M, Hammel J, Maldonado M, Müller WE, Nickel M, Schierwater B, Vacelet J, Wiens M, Wörheide G (2013) Deep metazoan phylogeny: when different genes tell different stories. Mol Phylogenet Evol 67:223–233

Philippe H, Derelle R, Lopez P, Pick K, Borchiellini C, Boury-Esnault N, Vacelet J, Renard E, Houliston E, Quéinnec E, Da Silva C, Wincker P, Le Guyader H, Leys S, Jackson DJ, Schreiber F, Erpenbeck D, Morgenstern B, Wörheide G, Manuel M (2009) Phylogenomics revives traditional views on deep animal relationships. Curr Biol 19:706–712

Redmond NE, Morrow CC, Thacker RW, Diaz MC, Boury-Esnault N, Cárdenas P, Hajdu E, Lôbo-Hajdu G, Picton BE, Pomponi SA, Kayal E, Collins AG (2013) Phylogeny and systematics of Demospongiae in light of new small-subunit ribosomal DNA (18S) sequences. Integ Comp Biol 53:388–415

Richards GS (2010) The origins of cell communication in the animal kingdom: notch signalling during embryogenesis and metamorphosis of the demosponge *Amphimedon queenslandica.* PhD Thesis The University of Queensland

Richards GS, Degnan BM (2012) The expression of Delta ligands in the sponge *Amphimedon queenslandica* suggests an ancient role for Notch signaling in metazoan development. EvoDevo 3:e15

Richards GS, Simionato E, Perrron M, Adamska M, Vervoort M, Degnan BM (2008) Sponge genes provide new insight into the evolutionary origin of the neurogenic circuit. Curr Biol 18:1156–1161

Rivera AS, Ozturk N, Fahey B, Plachetzki DC, Degnan BM, Sancar A, Oakley TH (2012) Blue-light-receptive cryptochrome is expressed in a sponge eye lacking neurons and opsin. J Exp Biol 215:1278–1286

Robinson JM, Sperling EA, Bergum B, Adamski M, Nichols SA, Adamska M, Peterson KJ (2013) The identification of microRNAs in calcisponges: independent evolution of microRNAs in basal metazoans. J Exp Zool B Mol Dev Evol 320:84–93

Ryan JF, Pang K, Schnitzler CE, Nguyen AD, Moreland RT, Simmons DK, Koch BJ, Francis WR, Havlak P, NISC Comparative Sequencing Program, Smith SA, Putnam NH, Haddock SH, Dunn CW, Wolfsberg TG, Mullikin JC, Martindale MQ, Baxevanis AD (2013) The genome of the ctenophore *Mnemiopsis leidyi* and its implications for cell type evolution. Science 342:1242592

Sakarya O, Armstrong KA, Adamska M, Adamski M, Wang IF, Tidor B, Degnan BM, Oakley TH, Kosik KS (2007) A post-synaptic scaffold at the origin of the animal kingdom. PLoS ONE 2:e506

Saller U, Weissenfels N (1985) The development of Spongilla lacustris from the oocyte to the free larva (Porifera, Spongillidae). Zoomorph 105:252–277

Schierwater B, Eitel M, Jakob W (2009) Concatenated analysis sheds light on early metazoan evolution and fuels a modern "urmetazoon" hypothesis. PLoS Biol 7:e20

Sebé-Pedrós A, Ariza-Cosano A, Weirauch MT, Leininger S, Yang A, Torruella G, Adamski M, Adamska M, Hughes TR, Gómez-Skarmeta JL, Ruiz-Trillo I (2013) Early evolution of the T-box transcription factor family. Proc Natl Acad Sci U S A 110: 16050–16055

Simpson TL (1984) The cell biology of sponges. Springer, New York

Sperling EA, Peterson KJ, Pisani D (2009) Phylogenetic-signal dissection of nuclear housekeeping genes supports the paraphyly of sponges and the monophyly of Eumetazoa. Mol Biol Evol 26:2261–2274

Srivastava M, Simakov O, Chapman J, Fahey B, Gauthier ME, Mitros T, Richards GS, Conaco C, Dacre M, Hellsten U, Larroux C, Putnam NH, Stanke M, Adamska M, Darling A, Degnan SM, Oakley TH, Plachetzki DC, Zhai Y, Adamski M, Calcino A, Cummins SF, Goodstein DM, Harris C, Jackson DJ, Leys SP, Shu S, Woodcroft BJ, Vervoort M, Kosik KS, Manning G, Degnan BM, Rokhsar DS (2010a) The *Amphimedon queenslandica* genome and the evolution of animal complexity. Nature 466:720–726

Srivastava M, Larroux C, Lu DR, Mohanty K, Chapman J, Degnan BM, Rokhsar DS (2010b) Early evolution of the LIM homeobox gene family. BMC Biol 8:e4

Steinmetz PRH, Kraus JEM, Larroux C, Hammel JU, Amon-Hassenzahl A, Houliston E, Wörheide G, Nickel M, Degnan BM, Technau U (2012) Independent evolution of striated muscles in cnidarians and bilaterians. Nature 487:231–234

Thacker RW, Freeman CJ (2012) Sponge-microbe symbioses: recent advances and new directions. Adv Mar Biol 62:57–111

Thacker RW, Hill AL, Hill MS, Redmond NE, Collins AG, Morrow CC, Spicer L, Carmack CA, Zappe ME, Pohlmann D, Hall C, Diaz MC, Bangalore PV (2013) Nearly complete 28S rRNA gene sequences confirm new hypotheses of sponge evolution. Integ Comp Biol 53:373–387

Tuzet O (1973) Éponges calcaires. In: Grassé P-P (ed) Traité de Zoologie Anatomie, Systématique, Biologie Spongiaires, vol 3. Masson et Cie, Paris, pp 27–132

Worheide G, Dohrmann M, Erpenbeck D, Larroux C, Maldonado M, Voigt O, Borchiellini C, Lavrov DV (2012) Deep phylogeny and evolution of sponges (phylum Porifera). Adv Mar Biol 61:1–78

Zakrzewski A-C, Weigert A, Helm C, Adamski M, Adamska M, Bleidorn C, Raible F, Hausen H (2014) Early divergence, broad distribution and high diversity of animal chitin synthases. Genome Biol Evol 6:316–325